OPTIMAL EFFICIENCY FIELD ORIENTED CONTROL OF AN INDUCTION MACHINE

by

SUNG CHUL OH

A DISSERTATION PRESENTED TO THE GRADUATE SCHOOL
OF THE UNIVERSITY OF FLORIDA IN PARTIAL FULFILLMENT
OF THE REQUIREMENTS FOR THE DEGREE OF
DOCTOR OF PHILOSOPHY

UNIVERSITY OF FLORIDA

1989

ACKNOWLEDGMENTS

I would like to express my deepest gratitude to my advisor and committee chairman, Professor Dennis P. Carroll, for his guidance, encouragement and support. I would also like to thank other professors, G. Basile, R. L. Sullivan, A. Domijan and B. Capehart for serving on my supervisory committee. I am also very grateful to the Korea Electrotechnology Research Institute for support. I would like to thank my parents and wife for their sincere support.

TABLE OF CONTENTS

page

ACKNOWLEDGMENT ii

NOMENCLATURE v

ABSTRACT vii

CHAPTERS

1 INTRODUCTION 1

2 REVIEW OF LITERATURE 9

3 FIELD ORIENTED CONTROL OF AN INDUCTION MACHINE 16

- 3.1 Mathematical Model of an Induction Machine 16
- 3.2 Basic Concept of Field Oriented Control 22
- 3.3 Implementation of Field Oriented Controller .25
- 3.4 Current Regulated Inverter 32

4 IDENTIFICATION OF ROTOR RESISTANCE 35

- 4.1 The Influence of Machine Parameter Deviation 35
- 4.2 Rotor Resistance Identification Method with MRAS 41

5 OPTIMAL EFFICIENCY CONTROL OF AN INDUCTION MACHINE . . 50

- 5.1 Analysis of Induction Machine Losses 50
- 5.2 Rotor Flux Selection for the Optimal Efficiency Control 53
- 5.3 Theoretical Results 55
- 5.4 Proposed Optimal Efficiency Control 60

6 SYSTEM SIMULATION 62

6.1 Test of FOC Alone 63
6.2 Test of Rotor Resistance Identifier 68
6.3 Full System Tests 71
6.4 Overall Controller Characteristics 78

7 SUMMARY AND CONCLUSIONS 83

APPENDIX 86

REFERENCES 89

BIOGRAPHICAL SKETCH 94

NOMENCLATURE

$\vec{v}_{abcs}$: abc phase stator voltage vector

$\vec{v}_{abcr}$: abc phase rotor voltage vector

$\vec{i}_{abcs}$: abc phase stator current vector

$\vec{i}_{abcr}$: abc phase rotor current vector

$\vec{\lambda}_{abcs}$: abc phase stator flux linkage vector

$\vec{\lambda}_{abcr}$: abc phase rotor flux linkage vector

r_s : Stator resistance

r_r : Rotor resistance

$\bar{r}_s$: Diagonal stator resistance matrix

$\bar{r}_r$: Diagonal rotor resistance matrix

L_{ms} : Magnetizing inductance of stator winding

L_{mr} : Magnetizing inductance of rotor winding

L_{sr} : Amplitude of the mutual inductance between stator and rotor windings

L_{ls} : Stator leakage inductance

L_{lr} : Rotor leakage inductance

θ_r : Rotor angular position

T_e : Electromagnetic torque

T_L : Load torque

J : Inertia of the rotor

ω_r : Angular speed of rotor

ω_e : Angular speed of source frequency

P : Number of poles

$\vec{v}_{qd0s}$: $qd0$ axis stator voltage vector

$\vec{v}_{dq0r}$: $qd0$ axis rotor voltage vector

$\vec{i}_{qd0s}$: $qd0$ axis stator current vector

$\vec{i}_{dq0r}$: $qd0$ axis rotor current vector

$\vec{\lambda}_{qd0s}$: $qd0$ axis stator flux linkage vector

$\vec{\lambda}_{qd0r}$: $qd0$ axis rotor flux linkage vector

$L_m = 1.5L_{ms}$: Magnetizing inductance

$L_s = L_{ls} + L_m$: Stator self inductance

$L_r = L_{lr} + L_m$: Rotor self inductance

$\omega_s = \omega_e - \omega_r$: Angular slip frequency

v_{qs}, v_{ds} : Stator voltages in q, d axis

i_{qs}, i_{ds} : Stator currents in q, d axis

v_{qr}, v_{dr} : Rotor voltages in q, d axis

i_{qr}, i_{dr} : Rotor currents in q, d axis

$\vec{i}_f$: Magnetizing current

$T_r = L_r/r_r$: Rotor time constant

r_m : Core loss resistor

Abstract of Dissertation Presented to the Graduate School
of the Unversity of Florida in Partial Fulfillment of the
Requirements for the Degree of Doctor of Philosophy

OPTIMAL EFFICIENCY FIELD ORIENTED CONTROL OF AN INDUCTION MACHINE

by

SUNG CHUL OH

May 1989

Chairman: Professor D. P. Carroll
Major Department: Electrical Engineering

A new control scheme for an induction machine is proposed. Optimal efficiency operation is achieved by adjusting rotor flux level using an indirect field oriented controller, which requires an accurate value of rotor resistance to calculate the slip command. The rotor resistance value used in the controller is continuously updated by a rotor resistance identifier, which uses a single-input-single-output (SISO) model reference adaptive system (MRAS) for rotor resistance identification. The proposed identifier requires only stator currents and rotor speed measurement. Because these measurements are also required in the field oriented controller, the need for additional measurement is obviated. For a given operating condition, the optimal rotor flux is calculated by an optimal flux selector, based on an equivalent circuit of the induction machine which includes a core loss resistor and the rotor resistance from the resistance identifier. The proposed optimal efficiency controller with rotor resistance identifier and optimal rotor flux selector is simulated with the Electro-Magnetic Transient Program (EMTP). Simulation results show excellent transient characteristics with the identifier and also verify the optimal efficiency operation of the induction machine by measuring input power.

CHAPTER 1

INTRODUCTION

Since the torque and flux of a dc machine can be controlled by adjusting the armature and field currents, respectively, dc machines have been used extensively in variable speed applications. However, the dc machine has following disadvantages in application.

- It is expensive compared to an ac machine.
- Existence of commutator and brush requires periodical maintenance.
- It cannot be used in an explosive or corrosive atmosphere.
- Commutator has limited capability in high speed and high voltage operation.

To overcome these problems, employing an induction machine in variable speed operation has received wide attention. Conventionally the induction machine has been used in fixed speed operation, in which speed is governed by the frequency of sinusoidal voltage waves. The induction machine can be used in variable speed operation with a power converter, which is an interface between the primary power supply and the induction machine. Although the ac machine (especially the squirrel cage type induction machine) is more rugged, reliable and inexpensive, the cost of the converter and control is considerably higher than that for a dc machine. But as new technology in power electronics is developed, the cost of converters will decrease and the performance will improve significantly. Control of the induction machine is a very complex task because of intricate coupling between control inputs and inner quantities like flux and torque. A complicated control strategy can be implemented with a micro-computer system, which provides hardware simplification and performance optimization. Since ac machines consume the majority of energy in a power system, potential energy saving is also expected with the variable speed ac drive system.

Since Blaschke [1] introduced the concept of field oriented control (FOC), there has been much research on the implementation of this concept. Most of the research focused on the analysis and design of the field oriented controller with various converters. In Chapter 2, literature concerning the various aspects of field oriented control of the induction machine is reviewed.

In Chapter 3, first a mathematical model of the induction machine is derived. Then based on this mathematical model, the basic concept of field oriented control and its implementation are presented. Field oriented control is also called vector control or transvector control.

The stator and rotor voltage equations of an induction machine can be transformed to the rotating reference frame which rotates at arbitrary speed [2, 3]. In rotating reference frame theory, any machine variable can be transformed to the arbitrary reference frame. In synchronous machine analysis, the rotor reference frame which rotates at the speed of the rotor is widely used. The synchronously rotating reference frame which rotates at the speed of the source frequency is suitable in induction machine analysis . The stator and rotor voltage equations transformed to the synchronously rotating frame are useful in finding the dynamic characteristics of the induction machine. The time varying coefficients appearing in the voltage equation in the abc machine variables can be eliminated after these equations are transformed to the synchronously rotating frame. If the machine is in steady state, machine voltage and current in the synchronously rotating reference frame are represented as dc values.

The basic concept of the field oriented control can be derived from the induction machine equations expressed in the synchronously rotating reference frame. If it is assumed that the reference frame is aligned with the rotor flux and the stator current can be controlled instantaneously, the torque equation is analogous to that of a separately excited dc machine. Torque can be represented as the multiplication of the rotor flux and the torque component of the stator current. Similar control strategies adopted for the dc machine can then be used in the induction machine control, i.e. by keeping the flux at a maximum level, the torque can be controlled instantaneously by adjusting the armature curent. It has been verified that excellent dynamic performance of an induction machine can be achieved with FOC [4]. In the field oriented control, the stator current should be controlled as vector quantity with torque and flux components.

In implementing the field oriented controller for the given torque and flux command, the reference value of the torque and flux component will be determined as a function of the machine parameters (rotor and magnetizing inductance). Reference values of each component should be transformed to the three-phase reference stator currents, which are reference values to the inverter. For the transformation, angular position of the rotor flux with respect to the stator axis (i.e. angular position of rotating frame) should be estimated or detected. Field oriented control can be classified into three catagories depending on the way the angular position of the rotor flux is determined:

1) Direct sensing method [5, 6] — Air-gap flux is measured by a sensing device like a Hall effect sensor. Rotor flux is calculated from the voltage equations of the stator and the measured air gap flux.

2) Indirect sensing method [4] — To avoid mounting a sensor, the rotor flux vector is calculated from the stator current and voltage which are measured by a sensing coil.

3) Indirect method [7] — The angular position of the rotor flux is estimated from the measured rotor speed and the slip frequency command, which is calculated from the reference values of torque and flux component of the stator current. This method is also called slip frequency control.

The above methods have various advantages and disadvantages. The direct sensing method is the ideal method to determine the angular position of rotor flux, but it requires an additional sensing device, which changes the basic structure of the induction machine and requires additional cost. The indirect sensing method suffers from an inaccuracy of flux estimation at the low speed region, arising from the inaccuracy of integration in low speed region.

In order to achieve the instantaneous control of the stator current among the various kinds of the converters, the current regulated pulse-width modulated (CRPWM) inverter is widely used. There are two main types of CRPWM inverters. One operates with hysteresis regulator and the other with a sine-triangle comparison regulator, which employs a natural sampling PWM algorithm with proportional integral (PI) compensation. The sine-triangle comparison regulator is widely used.

In Chapter 4, the necessity of rotor resistance identification is discussed and a new rotor resistance identifier is proposed. Because of its simplicity in determining the angular position of rotor flux, the indirect method is the most popular method in implementing the field oriented control. In the indirect method, the only required measurement is the rotor speed, which can be measured by a tachometer. The angular speed of the rotor flux is the sum of the measured rotor speed and the slip frequency command which is calculated by the required torque and flux components of stator current. The slip frequency command is a function of the rotor time constant. The performance of the indirect method depends on the accuracy of the machine parameters used in the controller. In order to generate the reference values of torque and flux components of the stator current, the rotor and magnetizing inductance value in the controller should be equal to the actual value. However, actual inductance will change with saturation. Meanwhile, in order to generate the slip frequency command, also the rotor time constant, which is a function of rotor inductance and rotor resistance, should also be equal to the actual value. Unfortunately the rotor time constant (in particular the rotor resistance) will change with temperature during operation. Using inaccurate machine parameters in the controller leads to undesirable transient and steady state error [8].

Ideally all the machine parameters in the indirect field oriented controller should be changed as the real machine parameters change. However, the key parameter experiencing the largest change is the rotor resistance, which is used in calculating the slip frequency command. In order to achieve accurate indirect field oriented control, change of rotor resistance should be detected or estimated. There are already several methods for rotor resistance identification. These methods use the principle that any change in machine parameters (especially rotor resistance) would effect certain machine variables. Garces [9] and Koyama et al. [10] defined a modified reactive power which is used as a criterion in the identification . Ohtani [11] used an airgap flux level as a criterion. Since the above methods focused on the steady state rotor resistance, the identified value is not suitable in the field oriented controller, which is based on a dynamic model.

Application of modern control theory to the rotor resistance identification encounters many difficulties, because of the nonlinear characteristic between input and output variables. But the field oriented controlled induction machine can be represented as a second order linear system with time varying coefficients. Model reference adaptive system (MRAS) can be used in tracking time varying parameters [12]. For the formulation, the process to be identified represents the actual induction machine which is operated with FOC, and the adaptive system is the mathematical model whose coefficients can be updated by the identification algorithm [13, 14]. Among the various implementations of MRAS, the output error method with state variable filter, which is required for a stable identification, is adopted in this dissertation. Since the new proposed method needs only a single input and single output measurement, additional measuring devices as in Sugimoto's method [13] is not necessary and thus the controller has a simple structure. Since the system model is based on the differential equation of the rotor flux, the identifier will work properly when there is a change in the machine operation.

In Chapter 5, various aspects of induction machine losses and the selection of optimal rotor flux levels in the field oriented controller are discussed. Finally, a new optimal efficiency controller is proposed, which utilizes FOC and a rotor resistance identifier.

Since electric machines in general, and induction machines in particular, consume a large fraction of all electrical power, problems related to the efficiency of induction machines have received wide attention. The losses in an induction machine can be reduced by the following method [15]:

1) Machine selection and design.

2) Improvement in the waveforms of the machine power supply. This involves the use of waveform shaping techniques for reducing the harmonics in the voltage and current delivered by inverters to the induction machine.

3) Adjusting voltage, current and/or frequency at each speed and torque operating point.

Chapter 5 will concentrate on method 3). Conventionally the air-gap flux of the induction machine is maintained at a rated value throughout the whole speed range, thus the torque sensitivity per ampere of stator current is maximum. With this method fast transient response system at all supply frequencies can be achieved. Rated value of air-gap flux is maintained by constant volt/hertz control with a variable-voltage-variable-frequency power supply. But it is found that in some conditions the air-gap flux is greater than necessary for the development of the required torque, which increases machine loss, and therefore the machine efficiency is reduced.

The efficiency of the induction machine can be improved by reducing air-gap flux. The purpose of this flux reduction is to maintain a better balance between load dependent losses (i.e. stator and rotor losses) and the load independent losses (i.e. core losses). The air-gap flux can be controlled over the complete torque and speed range by enforcing a precalculated relation between stator current, slip frequency and speed [16]. The disadvantage of this method is that, in order to get the relations between machine variables (e.g., stator currrent, slip frequency), accurate machine parameters need to be estimated.

A more direct method for optimal efficiency control of the induction machine, which utilizes FOC was recently developed by Kirschen et al. [17]. This method is based on the adaptive adjustment of rotor flux level using a field oriented controller and direct measurement of power input to the drive system. This method doesn't require knowledge of machine parameters, but it has the following disadvantages:

- It requires additional input power measurement devices like a wattmeter.
- Convergence to optimal efficiency is slow.
- If the condition of machine operation is changed (like sudden load change), optimal efficiency control may not be reached.

Efficiency of the induction machine can also be improved by adjusting the rotor flux level, which can be controlled directly with the field oriented controller, instead of controlling air-gap flux. In order to apply the FOC to the proposed optimal efficiency control, the optimal rotor flux level can be precalculated for the given torque and speed command instead of adjusting rotor flux gradually. This calculated rotor flux level is used as an input command to the field oriented controller. Optimal rotor flux is decided based on the torque command, speed command and identified rotor resistance.

In this dissertation, a new optimal efficiency field oriented controller is proposed. The rotor resistance used in the controller is updated with the rotor resistance identifier. The optimal rotor flux level is decided by the given torque and speed command and estimated rotor resistance. Optimal rotor flux level is calculated based on the steady state equivalent circuit of the induction machine including frequency dependent core loss resistance. First, optimal slip frequency is calculated, which minimizes the total machine loss including the stator and rotor, iron and copper losses, based on the equivalent circuit. With the field oriented controller, slip frequncy can be controlled by the rotor flux level. The optimal rotor flux level is defined as the rotor flux level which generates optimal slip frequency.

The proposed new optimal efficiency, field oriented controller has following advantages:

- No requirement for additional sensing devices other than tachometer, for the rotor resistance identifier and optimal efficiency controller.
- Rotor resistance value used in the controller is updated by the rotor resistance identifier.
- Rotor resistance identifier can be used even if the machine experiences a sudden change of operation.
- Convergence to optimal efficiency operation is relatively fast.
- Optimal rotor flux level, which is the input command to the field oriented controller, is updated according to the identified rotor resistance.

In Chapter 6, various simulation results of the proposed controller are shown. It is useful to simulate the new technique on a digital computer prior to its hardware implementation. A general purpose program which includes the induction machine model and control system components can greatly facilitate the simulation. For this purpose, the proposed optimal efficiency controller was simulated using the Electro-Magnetic Transient Program (EMTP).

CHAPTER 2

REVIEW OF LITERATURE

General aspects of ac machine drives, including ac machine operation, converters for ac machines, modelling and simulation, and the control of induction machines are reviewed by Bose [18]. It is suggested that future application areas for ac drive systems include the following:

- Replacing most existing applications of variable speed dc drives by the corresponding ac drive system, which will eventually make dc drives obsolete.
- Apply adjustable speed ac drives to the presently used constant speed process control ac drive applications, thereby saving energy.

The new optimal efficiency controller of an induction machine proposed in this dissertation considers both of these aspects.

Blaschke [1] proposed the concept of field oriented control (FOC), which reduces the control dynamics of the induction machine to those of a separately excited dc machine. This can be achieved by controlling stator current as a vector quantity with a torque and flux component. The FOC is based on the induction machine equations in the synchronously rotating reference frame [2, 3].

Gabriel et al. [5] and Leonhard [6] suggested the direct sensing field oriented controller, which calculated angular position of rotor flux from measured air-gap flux and stator current. This method requires flux detectors like Hall sensors, and suffers from harmonics caused by slot ripples. The main disadvantages of this method are as follows:

- It is very difficult to design a filter to eliminate harmonics.
- Mounting the measurement device changes the structure of the induction machine. This machine would no longer be a standard induction machine which can be acquired directly from stock.
- Hall sensors are mechanically fragile elements.

Nabae et al. [7] proposed an indirect FOC method which controls the stator current as a vector quantity on the basis of slip frequency control. In this method, the torque and flux components of stator current are calculated corresponding to the flux and torque commands, on the basis of machine parameters (rotor and magnetizing inductance). For the implementation, angular position of the rotor flux is calculated based on the torque and flux component and rotor speed. Even though this method doesn't require an air-gap flux measurement device, it requires accurate machine parameters to estimate angular position of rotor flux.

Indirect FOC is widely used because of its simplicity, and analysis of indirect FOC was done by many researchers [19, 20]. Excellent dynamic characteristics were also shown by Hirose et al. [4], that is the torque of the induction machine can be changed to the command value without an overshoot transient.

Another method for the control of the induction machine, called field acceleration method (FAM) was proposed by Yamamura [21]. In the FAM approach, the reference three-phase stator current is calculated from the specially defined induction machine equivalent circuit for the required torque. In the FOC, the three-phase reference stator current was transformed from the d-q axis reference current. This transformation is based on the slip frequency command from the controller. Meanwhile in the FAM, each phase reference stator current is calculated based on the equivalent circuit. FAM does not require a transformation but it is not suitable for direct flux control [4, 22].

In the FOC, stator current should be controlled instantaneously according to the reference current. For this purpose, the current regulated pulsewidth modulated (CRPWM) inverter is widely used. This inverter uses a particular PWM technique to achieve instantaneous current control. Hysteresis controllers generates a random PWM switching pattern to achieve reference and feedback current correspondence [23]. A ramp comparison controller uses the natural sampled PWM technique to perform current regulation [6]. The analysis of the CRPWM inverter based on the synchronously rotating reference frame is done by Rowan and Kerkman [24]. In fact, the CRPWM inverter can be considered as a proportional integral (PI) current regulator in the analysis. Alashhab et al. [22] showed some of the characteristics of the FOC and FAM methods with a voltage source inverter. It was found that instantaneous control cannot be achieved with the voltage source converter. Lorenz et al. [25] attempted to apply the state variable feedback model to the FOC. Lorenz and Divan [26] presented a new approach for current regulation, based on the use of a discrete time delta modulator from discrete time nonlinear optimal control theory, which offers the potential for substantial improvement over the classical or state space linear system controller. Enjeti et al. [27] suggested a new current control scheme using programmed PWM switching patterns with harmonic elimination approach. The proposed scheme consists of an amplitude correction loop and a phase correction loop.

In indirect FOC, the slip frequency calculator includes the estimated value of the rotor resistance, which varies with the temperature. If the value of the rotor resistance used in the slip frequency calculator deviates from the correct value, decoupling of flux and torque is lost and both steady-state and transient response is degraded [8]. There are already several methods available for rotor resistance identification.

Garces [9] and Koyama et al. [10] proposed an identification method in which modified reactive power was defined and the difference between reference reactive power (based on the reference stator current from the controller) and detected reactive power (based on the measured stator voltage) is used for rotor resistance identification. Similar to Garces' method, Ohtani [11] used error between reference value of air gap flux (based on the reference stator current from the controller) and calculated air gap flux (based on the measured stator voltage and current) for the rotor resistance identification. Steady state and dynamic characteristics of both Garces' method and Ohtani's method were analyzed and compared by Krishnan and Pillay [28].

Nagase et al. [29] suggested a method which compensated for the slip frequency command by using the deviation between reference rotor flux value and the actual value. Irisa et al. [30] developed an identification method in which measured real and reactive input power, stator current and slip frequency at two different operating points were used to estimate the rotor resistance. Sivakumar [31] proposed a steady state multi-parameter tuning procedure based on a d-q axis reference frame in which the stator current is in phase with the q-axis. Lorenz [32] proposed a method of tuning machine parameters depending on the transient response of the rotor current and flux to a step change in torque command. Matsuo and Lipo [33] introduced a different approach in which by injecting the negative sequence components to the machine, the corresponding voltage is sensed and decomposed into its d-q component. By injecting the signal at two widely separated frequencies, rotor resistance can be uniquely derived. Sul [34] estimated the rotor resistance based on the terminal voltages, currents and rotor speed. Dalal and Krishnan [35] proposed the estimation of rotor resistance by using the estimated air gap power. Lorenz and Lawson [36] presented a straightforward approach for estimating and fully decoupling the rotor flux and rotor time constant terms in indirect field oriented controller. This approach is based on the measured stator current and voltage which results from the use of delta modulator current regulator. Deleroi et al. [37] attempted to define the transient values of the parameters by comparing the measured results for transient performance to the simulated one. Wang et al. [38] estimated the rotor time constant by observing the voltage transient that occurs when the test current is switched to dc. Since the above methods are focused on steady-state operation, they are not suitable for the implementation of the field oriented controller in which the parameters used in the controller need to be dynamically updated.

Application of modern control theory to the control of induction machines has many difficulties. One of the difficulties is the induction machine is a nonlinear multivariable system. However, if the induction machine is operated with the field oriented control, it can represented as second order, time varying, linear system. Tracking of the time varying machine parameters can be achieved by applying model reference adaptive system (MRAS). Stability consideration of MRAS can be found in Landau [12]. Recently, many researches have considered the application of MRAS to the rotor resistance identification [13, 14]. Sugimoto & Tamai [13] applied the MRAS to the linearized d-q axis rotor flux equation of the induction machine. In order to implement the identifier, both components of rotor flux should be estimated or detected. Ohnishi et al. [14] used discrete type MRAS for the rotor resistance identification. For the system model, they neglected the electrical transients and only used the mechanical equations for the identification.

MRAS can be used as the optimal speed regulator as in Kumamoto [39]. Tamai et al. [40] proposed the application of MRAS to the rotor speed identification of the induction machine. In order to implement the indirect field oriented controller, the mechanical speed sensor (like tachogenerator) can be replaced by the speed identifier. Zai and Lipo [41] employed the extended Kalman filter to estimate the rotor time constant by using measurement of the stator voltages and currents and rotor speed of the induction machine. Kubota et al. [42] proposed a method which compensates the slip frequency command using a state observer which estimates the rotor flux.

Previous work on the loss minimization of electric drives has focused on the loss minimization at every steady state speed and torque operating condition. Mohan [43] suggested a method which improved the efficiency in lightly loaded induction machines by changing the amplitude of applied voltage. Jian, Schmitz and Novotny [44] calculated various characteristic (minimum input current, minimum input power, minimum efficiency) optimal slip values. If the slip can be held to a specified value by varying the applied voltage, maximum efficiency can be achieved.

With a variable-voltage-variable-frequency power supply, frequency as well as applied voltege can be controlled to get maximum efficiency. Kusko and Galler [15] developed a method which calculated the optimal frequency for the given speed and calculated optimal voltage as a function of torque. Kirschen, Novotny and Suwanwisoot [45] showed that machine efficiency can be improved by controlling the air-gap flux for any operating point. Kim et al. [16] controlled the air gap flux by varying stator current and slip frequency with a current source inverter (CSI). The above methods require precise knowledge of machine parameters including the variation of the core losses with frequency for the optimal control law.

Air-gap flux can also be controlled by the rotor flux, which is the input command value of the FOC. Kirschen, Novotny and Lipo [17] suggested a method which adaptively adjusts the flux level in the machine based on a direct measurement of the power input to the drive. A field oriented controller was used for the rotor flux control. This method doesn't require any knowledge of machine parameters but the convergence to the optimal efficiency is relatively slow and it may not reach the optimal efficiency if there is a sudden change in the machine operation. Takahashi and Noguchi [46] suggested another efficiency optimization method. In this method, optimal stator flux level is used as a command to the controller, which has different structure than the conventional field oriented controller.

Before the hardware implementation of the proposed new controller, it is recommended to test the validity of new controller by a full simulation. For the simulation, a general purpose program like Electro-Magnetic Transient Program (EMTP) is preferrable. EMTP is a computer program for simulating electromagnetic, electromechanical, and control system transients on multiphase electric power systems. It was first developed as a digital computer counterpart to the analog Transient Network Analyzer (TNA). Many other capabilities have been added to EMTP, and the program has become widely used in the utility industry. For the machine controller simulation, EMTP has two outstanding features. First, it has the Universal Machine module (UM) which can provide the transient response involving the interaction of electric machines with an electric power grid, as well as the machine interaction with complex networks of mechanical components of the induction machine. Second, it has Transient Analysis of Control System (TACS) which is developed for simulating the dynamic interaction between control systems and/or machines. TACS was designed as a simulation tool that functions in ways similar to analog computers with algebraic and logical processors combined. TACS signals and EMTP electrical network variables (including UM variables) can be interfaced to form a hybrid EMTP-TACS interactive configuration [47]. Daboussi and Mohan [48] simulated a field oriented controlled induction machine with EMTP, however, the machine parameters were assumed constant.

CHAPTER 3

FIELD ORIENTED CONTROL OF AN INDUCTION MACHINE

3.1 Mathematical Model of an Induction Machine

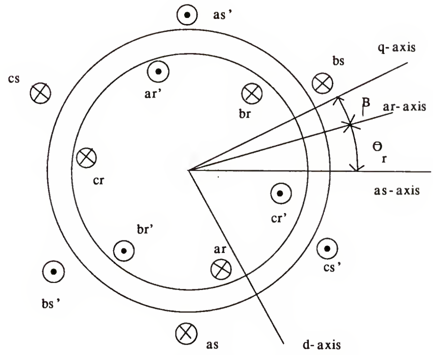

Fig. 3.1 Idealized 3–phase 2–pole induction machine

The induction machine is the most widely used electric motor and is characterized by its simple and rugged structure. The transient behavior of the induction machine is somewhat complicated because of the rotating field and the spatial relationships depending on speed and load. On the other hand the equivalent circuit usually derived for steady state operation is not suitable for the analysis of dynamic operation. The dynamic properties of an induction machine as a control plant can be described by a set of nonlinear differential equations linking the stator and rotor currents and voltages with the mechanical quantities like torque, speed and angular position.

Fig. 3.1 shows an idealized three-phase two-pole induction machine. The stator windings are identical, with assumed sinusoidally distributed windings displaced by 120°. Even in the squirrel cage induction machine, the rotor bars are arranged so that the rotor MMF wave can be considered to be a space sinusoid having the same number of poles as the stator MMF wave. The rotor windings are also considered as three identical sinusoidally distributed windings displaced by 120°.

The voltage equations in machine variables are expressed [3]

$$\vec{v}_{abcs} = \bar{r}_s \vec{i}_{abcs} + p\vec{\lambda}_{abcs} \qquad (3.1-1)$$

$$\vec{v}_{abcr} = \bar{r}_r \vec{i}_{abcr} + p\vec{\lambda}_{abcr} \qquad (3.1-2)$$

where s and r subscripts denote stator and rotor quantities, respectively. For a magnetically linear system the flux linkages may be expressed

$$\begin{bmatrix} \vec{\lambda}_{abcs} \\ \vec{\lambda}_{abcr} \end{bmatrix} = \begin{bmatrix} \bar{L}_s & \bar{L}_{sr} \\ \bar{L}_{sr}^t & \bar{L}_r \end{bmatrix} \begin{bmatrix} \vec{i}_{abcs} \\ \vec{i}_{abcr} \end{bmatrix} \qquad (3.1-3)$$

The winding inductances are defined as follows

$$\bar{L}_s = \begin{bmatrix} L_{ls} + L_{ms} & -\frac{1}{2}L_{ms} & -\frac{1}{2}L_{ms} \\ -\frac{1}{2}L_{ms} & L_{ls} + L_{ms} & -\frac{1}{2}L_{ms} \\ -\frac{1}{2}L_{ms} & -\frac{1}{2}L_{ms} & L_{ls} + L_{ms} \end{bmatrix} \qquad (3.1-4)$$

$$\bar{L}_r = \begin{bmatrix} L_{lr} + L_{mr} & -\frac{1}{2}L_{mr} & -\frac{1}{2}L_{mr} \\ -\frac{1}{2}L_{mr} & L_{lr} + L_{mr} & -\frac{1}{2}L_{mr} \\ -\frac{1}{2}L_{mr} & -\frac{1}{2}L_{mr} & L_{lr} + L_{mr} \end{bmatrix} \qquad (3.1-5)$$

$$\bar{L}_{sr} = L_{sr} \begin{bmatrix} \cos\theta_r & \cos\left(\theta_r + \frac{2\pi}{3}\right) & \cos\left(\theta_r - \frac{2\pi}{3}\right) \\ \cos\left(\theta_r - \frac{2\pi}{3}\right) & \cos\theta_r & \cos\left(\theta_r + \frac{2\pi}{3}\right) \\ \cos\left(\theta_r + \frac{2\pi}{3}\right) & \cos\left(\theta_r - \frac{2\pi}{3}\right) & \cos\theta_r \end{bmatrix} \qquad (3.1-6)$$

The torque equation is

$$T_e = \left(\frac{P}{2}\right)\left(\vec{i}_{abcs}\right)^t \frac{\partial}{\partial\theta_r}\left[\bar{L}_{sr}\right]\vec{i}_{abcr} \qquad (3.1-7)$$

where P is the number of poles and θ_r is the angle between rotor and stator magnetic axes. The electromagnetic torque T_e is related to the rotor speed ω_r and load torque T_L by the equation

$$T_e = J\left(\frac{2}{P}\right)p\omega_r + T_L \qquad (3.1-8)$$

where J is the rotor inertia constant.

As in (3.1–6), mutual inductance between the stator and rotor depends on θ_r, which varies as the machine rotates, as shown in Fig. 3.1. Therefore time varying inductance terms appear in the voltage equations (3.1–1) and (3.1–2). By transforming the voltage and current of both stator and rotor to a common reference frame, the time varying inductance terms can be eliminated. In the analysis of the induction machine, transformation of the machine variables to the synchronously rotating reference frame, which rotates at the source frequency, is widely used.

The transformation of the three-phase variables of the stator circuit to the synchronously rotating reference frame can be expressed in $qd0$ coordinates as [3]

$$\vec{f}_{qd0s} = \bar{K}_s\vec{f}_{abcs} \qquad (3.1-9)$$

$$\left(\vec{f}_{qd0s}\right)^t = \left[f_{qs} \quad f_{ds} \quad f_{0s}\right] \qquad (3.1-10)$$

$$\left(\vec{f}_{abcs}\right)^t = \left[f_{as} \quad f_{bs} \quad f_{cs}\right] \qquad (3.1-11)$$

$$\bar{K}_s = \frac{2}{3}\begin{bmatrix} \cos\theta_e & \cos\left(\theta_e - \frac{2\pi}{3}\right) & \cos\left(\theta_e + \frac{2\pi}{3}\right) \\ \sin\theta_e & \sin\left(\theta_e - \frac{2\pi}{3}\right) & \sin\left(\theta_e + \frac{2\pi}{3}\right) \\ \frac{1}{2} & \frac{1}{2} & \frac{1}{2} \end{bmatrix} \qquad (3.1-12)$$

$$\theta_e = \int_0^t \omega_e(\xi)\, d\xi + \theta_e(0) \tag{3.1 – 13}$$

In the above equations, f can represent either voltage, current, flux linkage, or electric charge and ω_e is the source frequency.

The transformation of the three-phase variables of the rotor circuit to the synchronously rotating reference frame can be expressed

$$\vec{f}_{qd0r} = \bar{K}_r \vec{f}_{abcr} \tag{3.1 – 14}$$

$$\left(\vec{f}_{qd0r}\right)^t = \left[\, f_{qr} \quad f_{dr} \quad f_{0r} \,\right] \tag{3.1 – 15}$$

$$\left(\vec{f}_{abcr}\right)^t = \left[\, f_{ar} \quad f_{br} \quad f_{cr} \,\right] \tag{3.1 – 16}$$

$$\bar{K}_r = \frac{2}{3}\begin{bmatrix} \cos\beta & \cos\left(\beta - \frac{2\pi}{3}\right) & \cos\left(\beta + \frac{2\pi}{3}\right) \\ \sin\beta & \sin\left(\beta - \frac{2\pi}{3}\right) & \sin\left(\beta + \frac{2\pi}{3}\right) \\ \frac{1}{2} & \frac{1}{2} & \frac{1}{2} \end{bmatrix} \tag{3.1 – 17}$$

$$\theta_r = \int_0^t \omega_r(\xi)\, d\xi + \theta_r(0) \tag{3.1 – 18}$$

$$\beta = \theta_e - \theta_r \tag{3.1 – 19}$$

where ω_r is a rotor speed.

By transforming the voltage equations (3.1–1) and (3.1–2) into the synchronously rotating reference frame with (3.1–9) and (3.1–14) respectively, the voltage equations become [3]

$$\vec{v}_{qd0s} = \bar{r}_s \vec{i}_{qd0s} + \omega_e \vec{\lambda}_{dqs} + p\vec{\lambda}_{qd0s} \tag{3.1 – 20}$$

$$\vec{v}_{qd0r} = \bar{r}_r \vec{i}_{qd0s} + (\omega_e - \omega_r)\, \vec{\lambda}_{dqr} + p\vec{\lambda}_{qd0r} \tag{3.1 – 21}$$

$$\vec{\lambda}^t_{dqs} = \begin{bmatrix} \lambda_{ds} & -\lambda_{qs} & 0 \end{bmatrix} \qquad (3.1-22)$$

$$\vec{\lambda}^t_{dqr} = \begin{bmatrix} \lambda_{dr} & -\lambda_{qr} & 0 \end{bmatrix} \qquad (3.1-23)$$

Transformation of the flux linkage equations (3.1–3) to the $qd0$ synchronous reference frame, using transformation matrices (3.1–12) and (3.1–17), gives

$$\begin{bmatrix} \vec{\lambda}_{qd0s} \\ \vec{\lambda}_{qd0r} \end{bmatrix} = \begin{bmatrix} \bar{K}_s\bar{L}_s\bar{K}_s^{-1} & \bar{K}_s\bar{L}_{sr}\bar{K}_r^{-1} \\ \bar{K}_r\bar{L}^t_{sr}\bar{K}_s^{-1} & \bar{K}_r\bar{L}_r\bar{K}_r^{-1} \end{bmatrix} \begin{bmatrix} \vec{i}_{qd0s} \\ \vec{i}_{qd0r} \end{bmatrix} \qquad (3.1-24)$$

$$\bar{K}_s\bar{L}_s\bar{K}_s^{-1} = \begin{bmatrix} L_{ls}+L_m & 0 & 0 \\ 0 & L_{ls}+L_m & 0 \\ 0 & 0 & L_{ls} \end{bmatrix} \qquad (3.1-25)$$

$$\bar{K}_r\bar{L}_r\bar{K}_r^{-1} = \begin{bmatrix} L_{lr}+L_m & 0 & 0 \\ 0 & L_{lr}+L_m & 0 \\ 0 & 0 & L_{lr} \end{bmatrix} \qquad (3.1-26)$$

$$\bar{K}_s\bar{L}_{sr}\bar{K}_r^{-1} = \bar{K}_r\bar{L}^t_{sr}\bar{K}_s^{-1} = \begin{bmatrix} L_m & 0 & 0 \\ 0 & L_m & 0 \\ 0 & 0 & 0 \end{bmatrix} \qquad (3.1-27)$$

where

$$L_m = \frac{3}{2}L_{ms} \qquad (3.1-28)$$

As we notice in (3.1–27), the time varying inductances are transformed to constant inductances.

The voltage equations (3.1–20) and (3.1–21) can be written in expanded form

$$v_{qs} = r_s i_{qs} + \omega_e \lambda_{ds} + p\lambda_{qs} \qquad (3.1-29)$$

$$v_{ds} = r_s i_{ds} - \omega_e \lambda_{qs} + p\lambda_{ds} \qquad (3.1-30)$$

$$v_{0s} = r_s i_{0s} + p\lambda_{0s} \qquad (3.1-31)$$

$$v_{qr} = r_r i_{qr} + (\omega_e - \omega_r)\,\lambda_{dr} + p\lambda_{qr} \qquad (3.1-32)$$

$$v_{dr} = r_r i_{dr} + (\omega_e - \omega_r)\lambda_{qr} + p\lambda_{dr} \qquad (3.1-33)$$

$$v_{0r} = r_r i_{0r} + p\lambda_{0r} \qquad (3.1-34)$$

Substituting (3.1–25)-(3.1–28) into (3.1–24) gives expressions for the flux linkages

$$\lambda_{qs} = L_{ls} i_{qs} + L_m (i_{qs} + i_{qr}) \qquad (3.1-35)$$

$$\lambda_{ds} = L_{ls} i_{ds} + L_m (i_{ds} + i_{dr}) \qquad (3.1-36)$$

$$\lambda_{0s} = L_{ls} i_{0s} \qquad (3.1-37)$$

$$\lambda_{qr} = L_{lr} i_{qr} + L_m (i_{qs} + i_{qr}) \qquad (3.1-38)$$

$$\lambda_{dr} = L_{lr} i_{dr} + L_m (i_{ds} + i_{dr}) \qquad (3.1-39)$$

$$\lambda_{0r} = L_{lr} i_{0r} \qquad (3.1-40)$$

Also the torque equation in (3.1–7) can be transformed to

$$T_e = \left(\frac{P}{2}\right) \left[\bar{K}_s^{-1} \vec{i}_{qd0s}\right]^t \frac{\partial}{\partial \theta_r} \left[\bar{L}_{sr}\right] \bar{K}_r^{-1} \vec{i}_{qd0r} \qquad (3.1-41)$$

Using the synchronously rotating reference frame is particularly convenient for the analysis of ac machines, since the voltage and current in this frame are constant during steady state operation and vary only when a system disturbance occurs. In the above equations, for balanced conditions, the 0–axis stator and rotor voltage equations can be neglected. In the case of a squirrel cage induction machine, since the rotor circuits are short-circuited, v_{qr} and v_{dr} are zero.

Therefore, the three-phase squirrel cage induction machine equations in the synchronously rotating reference frame can be written in the following matrix form, with balanced operation assumed

$$\begin{bmatrix} v_{qs} \\ v_{ds} \\ 0 \\ 0 \end{bmatrix} = \begin{bmatrix} r_s + L_s p & \omega_e L_s & L_m p & \omega_e L_m \\ -\omega_e L_s & r_s + L_s p & -\omega_e L_s & L_m p \\ L_m p & \omega_s L_m & r_r + L_r p & \omega_s L_r \\ -\omega_s L_m & L_m p & -\omega_s L_r & r_r + L_r p \end{bmatrix} \begin{bmatrix} i_{qs} \\ i_{ds} \\ i_{qr} \\ i_{dr} \end{bmatrix} \qquad (3.1-42)$$

where $L_s = L_m + L_{ls}$ is the stator self inductance, $L_r = L_m + L_{lr}$ is the rotor self inductance, $\omega_s = \omega_e - \omega_r$ is the slip frequency and p is the derivative operator. The torque equation can be written [2]

$$T_e = \frac{3}{2}\left(\frac{P}{2}\right) L_m \left(i_{qs} i_{dr} - i_{ds} i_{qr}\right) \qquad (3.1-43)$$

3.2 Basic Concept of Field Oriented Control

The induction machine as described by (3.1–42) and (3.1–43) is a much more difficult control plant compared to the dc machine. In the dc machine, the main flux and armature current can be controlled independently. But in the ac machine these quantities are strongly interacting and moving with respect to the stator as well as rotor, and they are determined by the amplitude, frequency and phase of the stator current. In addition, the rotor currents are inaccessible in a squirrel cage induction machine.

Variable speed operation of an ac machine can be realized with a converter. The block diagram of a conventional speed control system with constant volts/hertz control and slip regulation is shown in Fig. 3.2. The slip frequency ω_s^*, which is proportional to torque, is regulated by the speed loop error signal. The slip frequency ω_s^* is added to the rotor speed ω_r to generate the inverter frequency ω_e^*. The voltage reference v_e^* is calculated from ω_e^* through a function generator based on steady state operation so as to maintain airgap flux approximately constant. By keeping airgap flux at rated value, the torque sensitivity per ampere of current is maximum, which permits fast transient response of the system. The drive system accelerates with the clamped value of slip,

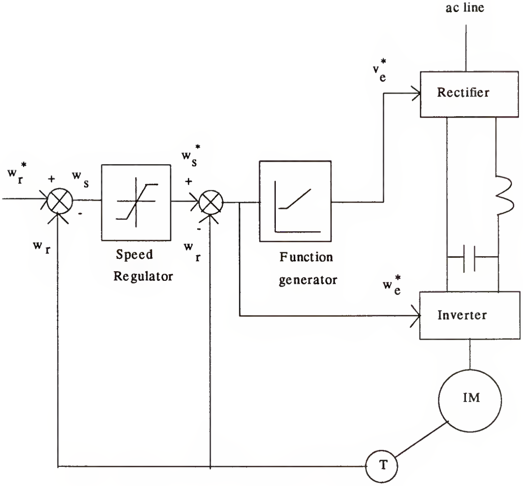

Fig. 3.2 Constant volts/hertz speed control with slip regulation

which may correspond to maximum torque, and then settles down to a value in steady-state conditions as dictated by the load torque. The above control scheme is not suitable for a high dynamic performance drive; therefore, it is preferred to use a control method which utilizes the dynamic model equations based on instantaneous current and voltage.

The concept of field oriented control was first introduced by Blaschke [1]. The idea is essentially to reduce the control dynamics of an ac machine to those of a separately excited dc machine. In a dc machine, the developed torque is given by $T_e = k_t I_f I_a$, where I_f is the field current and I_a is the armature current. The field current and armature current are mutually decoupled, and the best torque response can be obtained by controlling armature current while keeping the field current at rated value. In the ac machine, a similar analogy can be derived by using the flux component and the torque component of stator current, after transforming the stator current to a synchronously rotating frame that is aligned with rotor flux. It has been demonstrated that excellent dynamic performance of the induction machine can be achieved by field oriented control.

The basic concept of field oriented control is presented as follows. First we write (3.1–38) and (3.1–39) in the form

$$\vec{\lambda}_r = \begin{bmatrix} \lambda_{qr} \\ \lambda_{dr} \end{bmatrix} = \begin{bmatrix} L_r i_{qr} + L_m i_{qs} \\ L_r i_{dr} + L_m i_{ds} \end{bmatrix} \qquad (3.2-1)$$

where $\vec{\lambda_r}$ is rotor flux vector. Next we define the following new variables

$$\vec{i}_f = \begin{bmatrix} i_{qf} \\ i_{df} \end{bmatrix} = \begin{bmatrix} \lambda_{qr}/L_m \\ \lambda_{dr}/L_m \end{bmatrix} \qquad (3.2-2)$$

$$\vec{i}_a = \begin{bmatrix} i_{qa} \\ i_{da} \end{bmatrix} = \begin{bmatrix} i_{qf} - i_{qs} \\ i_{df} - i_{ds} \end{bmatrix} \qquad (3.2-3)$$

where $\vec{i_f}$ is defined as a magnetizing current vector. Assuming that the stator current can be controlled instantaneously, the stator voltage equations (first two rows of (3.1–42)) becomes a concern of the current controller. Therefore, these equations are not needed to solve for i_{qs} and i_{ds}, and can be eliminated from the model of the induction machine. That is, the stator current vector is considered to be an input to the control.

From the last two rows of (3.1–42) with new variables substituted from (3.2–1)-(3.2–3), the induction machine equations is may be written in the form

$$\begin{bmatrix} L_r & 0 \\ 0 & L_r \end{bmatrix} \begin{bmatrix} p i_{qf} \\ p i_{df} \end{bmatrix} + \begin{bmatrix} r_r & \omega_s L_r \\ -\omega_s L_r & r_r \end{bmatrix} \begin{bmatrix} i_{qf} \\ i_{df} \end{bmatrix} = \begin{bmatrix} r_r i_{qs} \\ r_r i_{ds} \end{bmatrix} \qquad (3.2-4)$$

$$T_e = \frac{3}{2}\left(\frac{P}{2}\right)\frac{L_m^2}{L_r}\left(i_{da}i_{qf} - i_{qa}i_{df}\right) \tag{3.2-5}$$

With the synchronous reference frame $d-$axis chosen to be in the same direction as the magnetizing current vector $\vec{i_f}$ in (3.2–2), i_{qf} becomes zero, so that (3.2–4) and (3.2–5) can be reduced to the desired FOC form, which resembles a separately excited dc machine.

$$T_r\frac{d}{dt}i_{df} + i_{df} = i_{ds} \tag{3.2-6}$$

$$\omega_e = \omega_r + \frac{1}{T_r}\frac{i_{qs}}{i_{df}} \tag{3.2-7}$$

$$T_e = \frac{3}{2}\left(\frac{P}{2}\right)\frac{L_m^2}{L_r}i_{df}i_{qs} \tag{3.2-8}$$

where $T_r = L_r/r_r$.

Once the transformation has been achieved, the dynamic structure of the induction machine is quite straightforward, not unlike that of a dc machine. In particular, there is a large time constant T_r comparable to the field lag of a dc machine. Therefore, the magnitude of the magnetizing current i_{df} is not available for fast control action influencing the torque. This task should be assigned to q-axis current i_{qs}. In order to obtain high dynamic performance of the induction machine, the same strategy as with the dc machine seems appropriate, i.e., the magnetizing current i_{df} should be maintained at maximum level, while torque should be controlled through i_{qs}.

3.3 Implementation of Field Oriented Controller

It was shown in the previous section that the induction machine can be controlled like a separately excited dc machine. For the given torque and flux command, reference values of the torque component (i_{qs}^*) and flux component (i_{ds}^*) of the stator current are calculated based on the induction machine equations in the synchronously rotating reference frame. The main assumption in the field oriented controller is that the d-axis of the synchronous rotating frame is aligned with the rotor flux. For the implementation of the controller, the reference values i_{qs}^* and i_{ds}^*, which are dc quantities, are transformed to a stationary reference frame with either the estimated or measured angular position of the rotor flux defined in (3.2–1). The resulting stationary values are then transformed to three-phase current commands for the inverter. Therefore, the accurate angular position of the rotor flux is necessary in the transformation. Fig. 3.3 explains the field oriented control principle with the help of a vector diagram. The stationary dq-axes are fixed on the stator, with the q-axis is aligned with the stator a-axis. The synchronous dq-axes rotate at synchronous angualar speed ω_e. At any instant, the synchronous q-axis is at angular position θ_e with respect to the stationary q-axis, i.e., θ_e is the angular position of the rotor flux (λ_r) with respect to stationary d-axis. Implementation of the field oriented controller can be divided into three catagories depending on the method of determining the angular position of the rotor flux, i.e., θ_e.

3.3.1 Direct Sensing Method

The magnitude and the angular position of the rotor flux is determined by the measured stationary air-gap fluxes λ_{dm}^s and λ_{qm}^s, which are measured by mounting two suitably spaced Hall sensors on the stator slots. One is aligned with the stator a-axis (i.e. stationary q-axis) and the other is aligned with the stationary d-axis, which lags the stationary q-axis by 90 °. By adding a voltage component proportional to the stator current vector, the rotor flux can be calculated. This is explained later in (3.3–3). If we compensate for the effect of the rotor leakage flux, the air-gap flux is equivalent to the rotor flux. The air-gap flux can be compensated for the rotor leakage as follows. First consider the d-axis rotor flux

$$\lambda_{dr}^s = L_m i_{ds}^s + L_r i_{dr}^s \qquad (3.3-1)$$

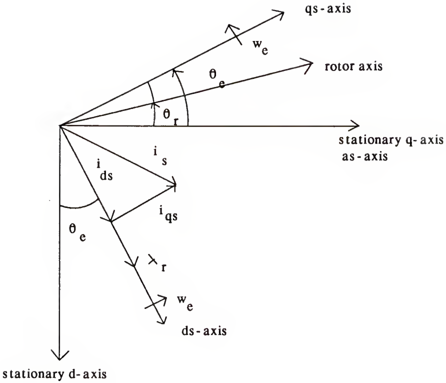

Fig. 3.3 Vector diagram for the field oriented contol

and from an equation similar to (3.1–36) written in the stationary reference frame, the mutual flux (second term) may be considered to be the air-gap flux

$$\lambda^s_{dm} = L_m i^s_{ds} + L_m i^s_{dr} \qquad (3.3-2)$$

where λ^s_{dr} is the d-axis rotor flux in the stationary reference frame, λ^s_{dm} is the measured air gap flux in the d-axis, and i^s_{ds}, i^s_{dr} are the $d-$axis stator and rotor current in the stationary reference frame. We must eliminate i^s_{dr} from (3.3–1), since in the squirrel cage induction machine, measuring the rotor current is impossible.

$$\lambda^s_{dr} = \frac{L_r}{L_m}\lambda^s_{dm} - L_{lr} i^s_{ds} \qquad (3.3-3)$$

Similarly, the q-axis rotor flux is

$$\lambda^s_{qr} = \frac{L_r}{L_m}\lambda^s_{qm} - L_{lr} i^s_{qs} \qquad (3.3-4)$$

The magnitude and angular position of rotor flux can then be given

$$|\lambda_r| = \sqrt{\lambda_{dr}^2 + \lambda_{qr}^2} = \sqrt{\left(\lambda^s_{dr}\right)^2 + \left(\lambda^s_{qr}\right)^2} \qquad (3.3-5)$$

$$\theta_e = \overset{-1}{\cos}\left(\frac{\lambda^s_{dr}}{|\lambda_r|}\right) \qquad (3.3-6)$$

where θ_e is an angle difference between the synchronous reference frame and the stationary reference frame. However, Hall sensors are mechanically fragile elements, which would not stand up very well under the severe vibrations and thermal stress. In addition, harmonics exist in the detected flux caused by slot ripples and saturation of the magnetic path. It is required to design filters to eliminate the harmonics, which is not an easy task. Another disadvange is this method changes the structure of the induction machine by installing sensors, which is no longer a standard induction machine available from stock. A block diagram of the direct sensing field oriented controller is shown in Fig. 3.4.

3.3.2 Indirect Sensing Method

This method is similar to the direct sensing method, but instead of mounting Hall effect sensors, the stationary reference frame value of rotor flux is calculated based on the measured stator voltage and current. That is, the machine terminal voltages and currents are used in estimating the rotor flux. The voltage equations of the induction machine in stationary reference frame have a similar form as (3.1–42). From (3.1–42), the voltage equations in the synchronous frame may be changed to the stationary reference frame by replacing ω_e with 0, and ω_s with $-\omega_r$. With the definition of the stator and rotor flux as in (3.1–35) and (3.1–38) and voltage equations in the stationary reference frame, the rotor flux in the stationary reference frame can be represented as follow.

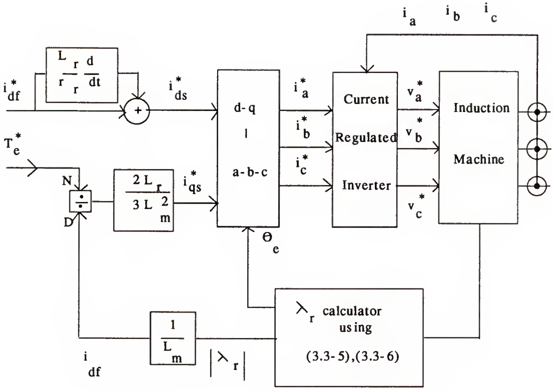

Fig. 3.4 Direct sensing FOC

$$\lambda_{dr}^s = (L_m - L_s L_r)\, i_{ds}^s + \frac{L_r}{L_m}\int \left(v_{ds}^s - r_s i_{ds}^s\right) dt \qquad (3.3-7)$$

$$\lambda_{qr}^s = (L_m - L_s L_r)\, i_{qs}^s + \frac{L_r}{L_m}\int \left(v_{qs}^s - r_s i_{qs}^s\right) dt \qquad (3.3-8)$$

Stationary reference frame values $i_{ds}^s, i_{qs}^s, v_{ds}^s, v_{qs}^s$ can be calculated from the measured three-phase voltages and currents. From the transformation matrix (3.1–12) with θ_e=0 for the stationary reference frame

$$\bar{K}_s^s = \frac{2}{3}\begin{bmatrix} 1 & -\frac{1}{2} & -\frac{1}{2} \\ 0 & -\frac{\sqrt{3}}{2} & \frac{\sqrt{3}}{2} \\ \frac{1}{2} & \frac{1}{2} & \frac{1}{2} \end{bmatrix} \qquad (3.3-9)$$

$$\vec{f}_{qd0s}^{\,s} = \bar{K}_s^s \vec{f}_{abcs} \qquad (3.3-10)$$

In balanced condition

$$f_{as} + f_{bs} + f_{cs} = 0 \qquad (3.3-11)$$

therefore

$$f_{qs}^{s} = f_{as} \qquad (3.3-12)$$

$$f_{ds}^{s} = \frac{1}{\sqrt{3}}(f_{cs} - f_{bs}) \qquad (3.3-13)$$

where f can be a voltage or current. The drawback of this method is that the stator resistance r_s must be compensated for temperature, which is important at low speed. In general, for reasonably high stator frequencies (above 10 Hz), there are only insignificant differences between actual flux and flux derived from the measured voltage and current. At lower frequencies, however calculated flux is much different from the actual flux, primarily because of unavoidable errors in $i_{dr}r_s, i_{qr}r_s$ terms. As the frequency is reduced voltages are small, thus any difference between the actual machine resistance and the nominal resistance value can create substantial measurement errors. The basic structure of the indirect sensing method is the same as in Fig. 3.4, but the stationary rotor flux values are estimated by using (3.3–7) and (3.8–8) from the measured stator voltage and current, rather than using (3.3–3) and (3.3–4).

3.3.3 Indirect Method

In this method, the required slip frequency command is calculated as shown below for the given torque and flux command. From (3.2–7) we get

$$\omega_s^* = \frac{1}{T_r}\frac{i_{qs}^*}{i_{df}^*} \qquad (3.3-14)$$

The angular positon of the rotor flux is decided by the measured rotor speed and slip frequency command, that is

$$\theta_e = \int_0^t (\omega_r + \omega_s^*)\, d\tau = \int_0^t \omega_e d\tau \qquad (3.3-15)$$

Because of its simplicity, the indirect method is widely used in implementing field oriented control. Indirect field oriented control is also called slip frequency control. The disadvantage of this method is that it requires knowledge of machine parameters. This method has the following advantages:

- Flux signals are not affected by the slot harmonics as in the direct sensing method.
- It can use a standard induction machine without additional sensors.
- Flux calculation is possible even in the low speed region.

The indirect field oriented controller is designed to calculate the reference components of stator current of the induction machine, corresponding to flux and torque commands on the basis of machine parameters (rotor and magnetizing inductance). These reference components are then transformed to the three-phase reference currents from the estimated angular position of rotor flux. A possible control strategy is as follows.

The torque command T_e^* and the magnetizing current command i_{df}^* are set to the desired value. The reference current i_{ds}^* from (3.2–6) is then

$$i_{ds}^* = T_r \frac{d}{dt} i_{df}^* + i_{df}^* \qquad (3.3-16)$$

and if i_{df}^* is constant, then $i_{ds}^* = i_{df}^*$. From (3.2–8), i_{qs}^* is

$$i_{qs}^* = \frac{2}{3}\left(\frac{2}{P}\right)\frac{L_r}{L_m^2}\frac{T_e^*}{i_{df}^*} \qquad (3.3-17)$$

Then the slip frequency ω_s^* from (3.2–7) is

$$\omega_s^* = \frac{1}{T_r}\frac{i_{qs}^*}{i_{df}^*} \tag{3.3 – 18}$$

The time–varying angular position of the rotor flux θ_e is determined by (3.3–15). This is also the angle between the synchronous and stationary reference frame, as indicated in Fig. 3.3.

With θ_e and the reference values i_{ds}^*, i_{qs}^* the reference phase currents i_a^*, i_b^*, i_c^* are calculated using the synchronous reference frame to $a-b-c$ frame transformation K_s^{-1} with zero quantities omitted for balanced operation,

$$\begin{bmatrix} i_a^* \\ i_b^* \\ i_c^* \end{bmatrix} = \begin{bmatrix} \cos\theta_e & \sin\theta_e \\ \cos\left(\theta_e - \frac{2\pi}{3}\right) & \sin\left(\theta_e - \frac{2\pi}{3}\right) \\ \cos\left(\theta_e + \frac{2\pi}{3}\right) & \sin\left(\theta_e + \frac{2\pi}{3}\right) \end{bmatrix} \begin{bmatrix} i_{qs}^* \\ i_{ds}^* \end{bmatrix} \tag{3.3 – 19}$$

A indirect field oriented controller applying the above control strategy is shown in Fig. 3.5.

3.4 Current Regulated Inverter

The main assumption of the field oriented control scheme is instantaneous control of the stator current. This method of stator current control can be realized through the use of a high gain PWM current amplifier, often referred to as a current regulated PWM (CRPWM) inverter. As discussed earlier, by employing such an CRPWM inverter in the control of an induction machine, stator dynamics can be eliminated. The CRPWM inverter can be classified as either a hysteresis or a ramp comparison regulator.

A hysteresis regulator utilizes some type of hysteresis in the comparison of the line currents to the current references. The hysteresis type CRPWM inverter is shown in Fig. 3.6, with a choice of suitable transistors having a fast switching time. By using a fast switching transistor, audio noise interference can be avoided. The main operation of the inverter is explained as follows, using phase 'a' for illustration. As the current exceeds

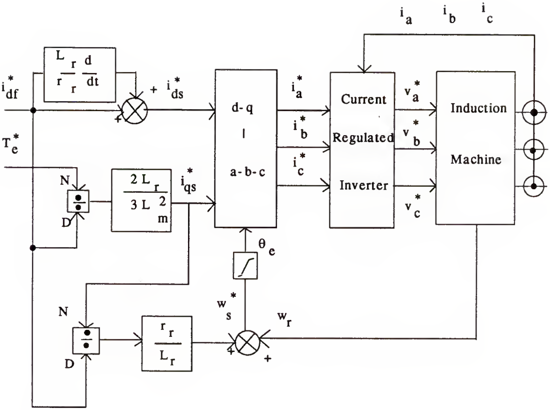

Fig. 3.5 Indirect FOC

a prescribed hysteresis band, the upper transistor (T1) is turned off and lower transistor (T4) is turned on. As a result, the current starts to decrease. As the current crosses the lower band limit, the upper transistor (T1) is turned on and lower transistor (T4) is turned off. The line current is thus forced to track the reference current within the desired hysteresis band. The inverter switching frequency will vary over a fundamental inverter period since the current ripple is specified by the hysteresis band.

The ramp comparison controller compares the current error to a triangle waveform to generate the inverter firing signals. This regulator can be considered as producing a sine-triangle PWM with the current error considered to be the modulation function. The current error is compared to a triangle waveform and if the current error is greater (less) than the triangle waveform, then the inverter leg is switched in the positive (negative) direction. In the sine-triangle PWM, the inverter switches at the frequency of the triangle wave. It

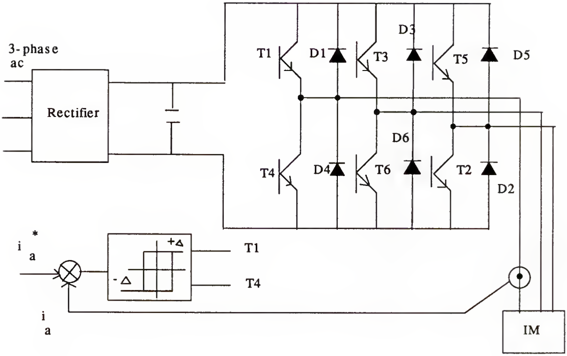

Fig. 3.6 Current regulated PWM inverter (hysteresis type)

has been shown there is an inherent magnitude and phase error in the actual current. This error can be reduced by increasing the controller gain or adding compensation. The gain of the controller can be adjusted by either adjusting the triangle amplitude or amplifying the current error. For the compensation, proportional integral (PI) type compensation is widely used. The time constant of the compensator should be set equal to the machine stator time constant [49].

CHAPTER 4

IDENTIFICATION OF ROTOR RESISTANCE

4.1 The Influence of Machine Parameter Deviation

The field oriented control (FOC) is used to obtain precise control of the inverter fed induction machine by transforming it to an equivalent separately excited dc machine. Crucial to the performance of the FOC is the knowledge of the instantaneous position of the rotor flux. This can be measured using either Hall probes or search coils. To accomplish this, modification to an existing machine with extra cost is required. In addition, flux measurement at low speed is difficult.

Therefore indirect FOC, which estimates the position of the rotor flux using a mathematical model of the machine, is the preferred implementation. In the indirect FOC method, accurate a priori knowledge of the induction machine parameters is needed to estimate the position of the rotor flux. But changes in temperature, current and synchronous frequency vary the machine parameters and hence indirectly influence operation of the induction machine. Ideally all model parameters used in the FOC should be modified as they change in the machine. It is difficult however to determine the change in every machine parameter.

As indicated in Fig. 3.5, the field oriented controller is dependent on three machine parameters: rotor resistance, magnetizing inductance and rotor self inductance. The inductances change with saturation, while rotor resistance is a function of machine temperature. Inductances change due to saturation of the iron magnetic paths, and this causes a problem in determining machine parameters. The problem then becomes nonlinear and its analytical treatment becomes difficult. However, in most cases influence of the saturation is small and negligible [21]. The parameters used in the field oriented controller model should be equal to the actual value in the induction machine. Ideally all the machine parameters in the indirect field oriented controller should be changed as the real machine parameters. The key paramater experiencing the largest change is the rotor resistance, which is used in calculating the slip frequency command. Any mismatch of parameters causes inaccurate commands of i_{qs}^*, i_{ds}^* and ω_s^*. This results in lower performance or undesirable oscillation in the rotor flux and electric torque.

The effects of the parameter mismatch (especially the rotor resistance value used in the controller) will now be examined. The field oriented controller is based on the induction machine equations in the synchronously rotating reference frame with d-axis aligned with the rotor flux. If $d-q$ axis currents are defined as complex components, phasor representation is possible.

$$\vec{i}_{qds} = i_{qs} - j i_{ds} = \vec{i}_s \tag{4.1-1}$$

$$\vec{i}_{qdr} = i_{qr} - j i_{dr} = \vec{i}_r \tag{4.1-2}$$

In the field oriented controller, two current commmands i_{qs}^* and i_{ds}^* are decided by the torque and flux commands respectively. The slip frequency command ω_s^* is calculated with the i_{qs}^* and i_{ds}^*, assuming the derivative term in (3.2–6) is negligible.

$$\omega_s^* = \frac{1}{T_r^*} \frac{i_{qs}^*}{i_{ds}^*} \tag{4.1-3}$$

where $T_r^* = L_r / r_r$. Considering i_{qs}^* and i_{ds}^* as input currents to the induction machine, we can derive the phasor relation between rotor and stator current from the last two rows of (3.1–42) by neglecting terms containing derivative operator p.

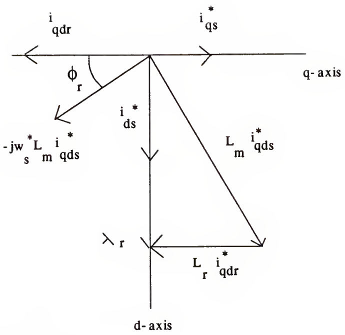

Fig. 4.1 Phasor diagram with correct value of slip calculator

$$\vec{i}_{qdr} = \frac{-j\omega_s^* L_m \vec{i}^*_{qds}}{r_r + j\omega_s^* L_r} \tag{4.1 - 4}$$

The reference current i^*_{qds} fixes the position of the flux linkage phasor $L_m i^*_{qds}$ which in turn fixes the position of the rotor induced voltage $-j\omega_s^* L_m i^*_{qds}$ as shown in Fig. 4.1. The phase angle of the rotor self-impedance $\phi_r = tan^{-1}\omega_s^* T_r$ locates the position of the rotor current i_{qdr}. If the reference rotor time constant T_r^* is equal to the actual rotor time constant T_r, the rotor current will be exactly in opposition to the torque command current i^*_{qs} and correct field orientation is achieved. The rotor flux λ_r will also be aligned with i_{ds}.

With an incorrect value of slip ω_s^*, due to an incorrect rotor time constant T_r^*, correct FOC cannot be achieved. This is illustrated in Fig. 4.2. In this example, the predicted rotor time constant is larger than the actual rotor time constant resulting in a smaller value of slip. This gives a shorter rotor induced voltage phasor $-j\omega_s^* L_m i_{qds}^*$ which remains in the same position. The rotor self impedance angle ϕ_r is also smaller because of the reduced slip. Thus the rotor current i_{qdr} will no longer line up with q-axis, but is pushed down towards the d-axis. The rotor flux will move away from the d-axis counterclockwise, as to maintain orthogonality with i_{qdr} and the alignment of rotor flux with the d-axis is disturbed. The phasor diagram also indicates an increase in the amplitude of rotor flux. When correctly aligned, the rotor flux equals $L_m i_{ds}$. However, with a change in i_{qdr} and hence $L_r i_{qdr}$, this is no longer true because $L_r i_{qdr}$ is not completely opposed by the quadrature component of $L_m i_{qds}^*$. This results in a q-axis and an additional d-axis component of rotor flux, and the rotor flux increases in magnitude [8].

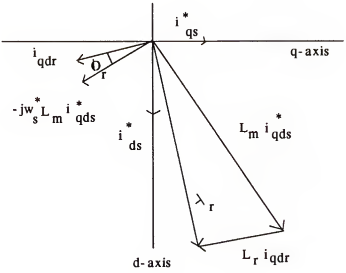

Fig. 4.2 Phasor diagram with incorrect slip calculator

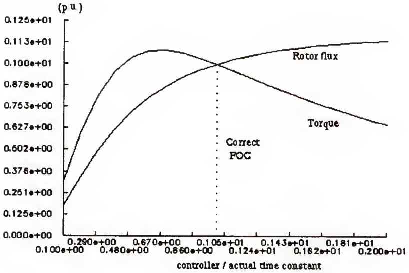

Fig. 4.3 Steady-state effect of slip calculator error for rated command current

If the reference rotor time constant T_r^* is smaller than the actual value, the slip command ω_s^* is larger than required to achieve correct FOC. In this case, the rotor induced voltage $-j\omega_s^* L_m i_{qds}^*$ remains in the same position and has a larger value. Thus the rotor current i_{qdr} will no longer be aligned with the $q-$axis, but is pushed above the $d-$axis. The rotor flux λ_r will move clockwise away from the $d-$axis with a smaller amplitude than that for the correct FOC.

Next we will examine the effects of errors in the slip calculator (4.1–3) for the steady state operation of the induction machine. Constant i_{qs}^* and i_{ds}^* commands are assumed corresponding to constant torque and flux commands. The steady state performance curves in terms of the rotor flux and output torque are shown in Fig. 4.3. The flux curve indicates that as the predicted time constant in the slip calculator gets larger compared to the actual value, the flux increases from its correct value while the output torque decreases. When the predicted time constant is less than the actual value, the rotor flux decreases with increase in error, while the torque output first increases then decreases as shown in Fig. 4.3.

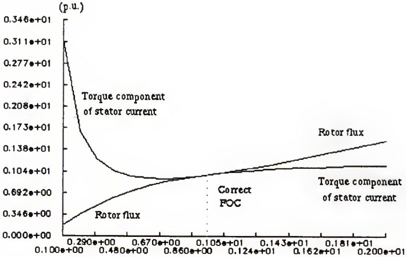

Fig. 4.4 Steady-state effect of slip calculator for constant torque output operation

The preceding situation of constant torque and constant flux operation is conceptually simple but is not representative of typical operation. A more normal operation would involve a speed control loop which would regulate the torque command current i_{qs}^* so as to obtain the torque necessary to meet the output speed requirement. This situation can be examined by finding the required torque command and flux which result from a slip calculator under a constant torque output constraint. Fig. 4.4 shows the results. In general, the required torque command current follows a curve which is roughly the inverse of the torque curve in Fig. 4.3.

In addition to changing the steady-state flux and torque, a rotor time constant error also effects the dymanic response associated with the field oriented control. In particular, the ideal instantaneous torque response to changes in the torque command is lost, because with the rotor time constant error there is both a flux and a torque response to the step change of torque command. The analysis of the transient response of a detuned system can be done by small signal analysis techniques. The transient response with incorrect slip command has been examined by forming the small-signal transfer function between the torque response and the torque command current. The transfer function $\Delta T_e/\Delta i_{qs}^*$

has the following properties [8] :

- A pair of complex poles with the real part equal to $-1/T_r$ and the imaginary part equal to the commanded slip frequency ω_s^*.
- A pair of complex zeros which exactly cancel the poles when $T_r = T_r^*$.
- A dc gain is agreement with (3.2–8) when $T_r = T_r^*$.

Note that only the real part of the pole is affected by the rotor time constant error. A large rotor time constant error may cause the pole to be closer to the imaginary axis and generally more poorly damped than for the correct FOC.

4.2 Rotor Resistance Identification Method with MRAS

The rotor time constant, in particular the rotor resistance r_r used in the field oriented controller should be updated during operation of machine. Since the rotor resistance changes with temperature, identification of rotor resistance is essential in the indirect field oriented control. There are already several methods available for rotor resistance identification. A representative method is to design the identifier in order to equalize the output of a mathematical model without rotor resistance, to that of a model with rotor resistance [28].

Tracking of machine parameters when they vary with time can be formulated as a model reference adaptive system (MRAS). The induction machine to be identified represents the reference model. The adjustable system is an adjustable model of the induction machine whose parameters are driven by an identification mechanism. There are three basic configurations depending on the configuration of the estimation model, the signals which are fed in, and how the error between the outputs of the process and the estimation model are obtained, these basic configurations are the output error method, equation error method, and input error method. The output error method was chosen here for the rotor resistance identification scheme.

The basic equations for the field oriented controlled induction machine given by (3.2–4) may be rewritten in the form

$$\begin{bmatrix} pi_{qf} \\ pi_{df} \end{bmatrix} = \begin{bmatrix} -\frac{r_r}{L_r} & -\omega_s \\ \omega_s & -\frac{r_r}{L_r} \end{bmatrix} \begin{bmatrix} i_{qf} \\ i_{df} \end{bmatrix} + \begin{bmatrix} \frac{r_r}{L_r} i_{qs} \\ \frac{r_r}{L_r} i_{ds} \end{bmatrix} \qquad (4.2-1)$$

with the field constraint from (3.2–6)

$$\omega_s = \frac{r_r}{L_r}\frac{i_{qs}}{i_{ds}} = \frac{1}{T_r}\frac{i_{qs}}{i_{ds}} \qquad (4.2-2)$$

where pi_{df} is assumed negligible. Substituting (4.2–2) into (4.2–1)

$$\begin{bmatrix} pi_{qf} \\ pi_{df} \end{bmatrix} = \begin{bmatrix} -\frac{1}{T_r} & -\omega_s \\ \omega_s & -\frac{1}{T_r} \end{bmatrix} \begin{bmatrix} i_{qf} \\ i_{df} \end{bmatrix} + \begin{bmatrix} \omega_s \\ \frac{1}{T_r} \end{bmatrix} i_{ds} \qquad (4.2-3)$$

The above equation represents the induction machine operating in FOC where the parameters ω_s and T_r are time varying values which will be identified by the adaptive system.

The single-input/single-output transfer function between i_{df} and i_{ds} can be derived from (4.2–3)

$$H(s) = \frac{i_{df}}{i_{ds}} = \frac{\frac{1}{T_r}s + \left(\frac{1}{T_r^2} + \omega_s^2\right)}{s^2 + \frac{2}{T_r} + \left(\frac{1}{T_r^2} + \omega_s^2\right)} \qquad (4.2-4)$$

Defining the new variables

$$a_1 = \frac{2}{T_r} \qquad (4.2-5)$$

$$a_0 = \frac{1}{T_r^2} + \omega_s^2 \qquad (4.2-6)$$

$$b_1 = \frac{1}{T_r} \qquad (4.2-7)$$

$$b_0 = \frac{1}{T_r^2} + \omega_s^2 \qquad (4.2-8)$$

(4.2–4) can be rewritten as

$$H(s) = \frac{b_1 s + b_0}{s^2 + a_1 s + a_0} \qquad (4.2-9)$$

The problem is to identify the time varying coefficients a_1, a_0, b_1, b_0, when the machine is operating with a given torque and flux command.

Only the input and output measurements i_{ds}, i_{df} will be used to implement the rotor resistance identifier for the single-input/single-output system. The output error method is shown in Fig. 4.5 for the rotor resistance identification. A state variable filter is placed before the mathematical model to insure a stable identifier, and another one is placed after the induction machine output to provide filtered derivatives of i_{df}. The need for these filters is explained later. The corresponding identifier will be described as follows [12].

Referring to Fig. 4.5, the model of the induction machine to be identified has the form given by (4.2–4)

$$\left(\sum_{i=0}^{2} a_i p^i\right) i_{df} = \left(\sum_{i=0}^{1} b_i p^i\right) i_{ds}, \ a_2 = 1 \qquad (4.2-10)$$

The state variable filter acting on the machine output is

$$\left(\sum_{i=0}^{1} c_i p^i\right) i_{mdf} = i_{df}, \ c_1 = 1 \qquad (4.2-11)$$

and the same type of filter acts on the model input is

$$\left(\sum_{i=0}^{1} c_i p^i\right) i_{sds} = i_{ds}, \ c_1 = 1 \qquad (4.2-12)$$

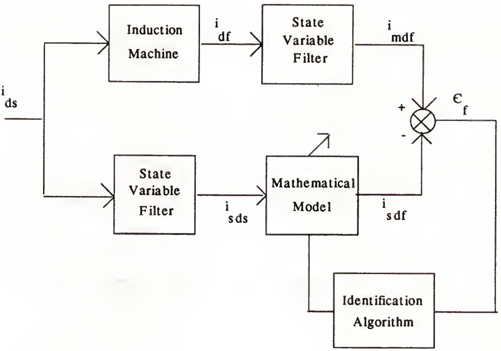

Fig. 4.5 Output error method

The mathematical model is in the same form as (4.2–10) with parameters that need to be identified

$$\left(\sum_{i=0}^{2} \hat{a}_i p^i\right) i_{sdf} = \left(\sum_{i=0}^{1} \hat{b}_i p^i\right) i_{sds}, \; \hat{a}_2 = 1 \qquad (4.2-13)$$

The filtered generalized error is

$$\epsilon_f = i_{mdf} - i_{sdf} \qquad (4.2-14)$$

The identification law is [12]

$$v = \left(\sum_{i=0}^{1} d_i p^i\right) \epsilon_f = D(p)\, \epsilon_f \qquad (4.2-15)$$

$$\hat{a}_i(v,t) = \int_0^t \phi_{1i}(v,t,\tau)\,d\tau + \phi_{2i}(v,t) + \hat{a}_i(0) \qquad (4.2-16)$$

$$\hat{b}_i(v,t) = \int_0^t \psi_{1i}(v,t,\tau)\,d\tau + \psi_{2i}(v,t) + \hat{b}_i(0) \qquad (4.2-17)$$

In the above equations p is the derivative operator.

The design objective in this case is :

1. Determine $D(p), \phi_{1i}, \phi_{2i}, \psi_{1i}, \psi_{2i}$ such that lim $\epsilon_f = 0$ for all initial conditions of $\hat{a}_i(0), \hat{b}_i(0)$ and for all input functions belonging to the class of piecewise continous functions.

2. Find the supplementary conditions which lead to

$$\lim_{t\to\infty} \hat{a}_i(v,t) = a_i \quad and \quad \lim_{t\to\infty} \hat{b}_i(v,t) = b_i$$

From (4.2–10), (4.2–11) and (4.2–12)

$$\left(\sum_{i=0}^{2} a_i p^i\right) i_{mdf} = \left(\sum_{i=0}^{1} b_i p^i\right) i_{sds}, \; a_2 = 1 \qquad (4.2-18)$$

where i_{sds} is the output of the state variable filter of (4.2–12). Adding the terms

$$\sum_{i=0}^{2} a_i p^i i_{sdf}$$

to both sides of (4.2–13) and then subtracting (4.2–13) from (4.2–18) one obtains

$$\left(\sum_{i=0}^{2} a_i p^i\right)\left(i_{mdf} - i_{sdf}\right) - \sum_{i=0}^{2} \hat{a}_i(v,t) p^i i_{sdf}$$
$$= -\left(\sum_{i=0}^{2} a_i p^i\right) i_{sdf} + \sum_{i=0}^{1}\left(b_i - \hat{b}_i(v,t)\right) p^i i_{sds} \qquad (4.2-19)$$

Also using (4.2–14), we get

$$\left(\sum_{i=0}^{2} a_i p^i\right) \epsilon_f = \sum_{i=0}^{2} \left(\hat{a}_i(v,t) - a_i\right) p^i i_{sdf} - \sum_{i=0}^{1} \left(\hat{b}_i(v,t) - b_i\right) p^i i_{sds} \qquad (4.2-20)$$

From (4.2–15) – (4.2–17) and (4.2–20), we obtain the following equivalent feedback system, noting that $a_2 = 1$ reduces the first summation in the right side of (4.2–20) to two terms, that is

$$\left(\sum_{i=0}^{2} a_i p^i\right) \epsilon_f = w_1 \qquad (4.2-21)$$

$$v = \left(\sum_{i=0}^{1} d_i p^i\right) \epsilon_f \qquad (4.2-22)$$

$$w = -w_1 = -\sum_{i=0}^{1} \left(\int_0^t \phi_{1i}(v,t,\tau)\, d\tau + \phi_{2i}(v,t) + \hat{a}_i(0) - a_i\right) p^i i_{sdf} + \sum_{i=0}^{1} \left(\int_0^t \psi_{1i}(v,t,\tau)\, d\tau + \psi_{2i}(v,t) + \hat{b}_i(0) - b_i\right) p^i i_{sds} \qquad (4.2-23)$$

where the linear feedforward block (with input w_1 and output v) is described by (4.2–21) and (4.2–22) and the time varying nonlinear feedback block (with input v and output w) is described by (4.2–23). This is illustrated in Fig. 4.6.

The identification algorithm from (4.2–15) - (4.2–17) must be chosen so that the equivalent nonlinear feedback system satisfies two conditions to realize the stable identification [12].

(1) The nonlinear time variant block satisfies the following Popov integral inequality

$$\int_0^t vw\,dt \geq -\gamma^2 \qquad (4.2-24)$$

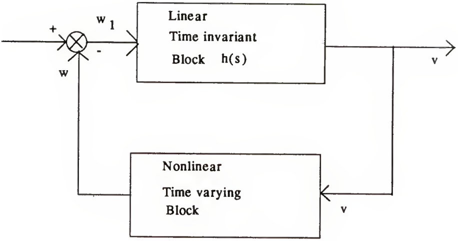

Fig. 4.6 Equivalent feedback system

where γ^2 is a positive constant. One of the possible solutions satisfying (4.2–24) is

$$\begin{aligned}
\phi_{1i} &= -k_{ai} v p^i i_{sdf} \\
\phi_{2i} &= -k'_{ai} v p^i i_{sdf} \\
\psi_{1i} &= k_{bi} v p^i i_{sds} \\
\psi_{2i} &= k'_{bi} v p^i i_{sds}
\end{aligned} \qquad (4.2-25)$$

where $k_{ai}, k'_{ai}, k_{bi}, k'_{bi} > 0$. The proportional integral identification law is then

$$\begin{aligned}
\hat{a}_i(v,t) &= -\int_0^t k_{ai} v p^i i_{sdf} d\tau - k'_{ai} v p^i i_{sdf} + \hat{a}_i(0) \\
\hat{b}_i(v,t) &= \int_0^t k_{bi} v p^i i_{sds} d\tau + k'_{bi} v p^i i_{sds} + \hat{b}_i(0)
\end{aligned} \qquad (4.2-26)$$

(2) The transfer function of the linear time invariant block should be strictly positive real. This is $h(s)$ in Fig. 4.6, and from (4.2–21) and (4.2–22) it can be expressed

$$h(s) = \frac{\sum_{i=0}^{1} d_i s^i}{\sum_{i=0}^{2} a_i s^i} = \frac{d_0 + d_1 s}{a_0 + a_1 s + s^2} \qquad (4.2-27)$$

To be strictly positive real, this transfer function must have the following properties [12]:

- $h(s)$ is real for real s.
- The poles of $h(s)$ should lie in the left hand complex plane, Re$[s] < 0$.
- For all real ω, one has Re$[h(j\omega)] > 0$.

For this specific application, a constant gain (i.e. $D(s) = d$) was tried, but it was impossible to get a positive real $h(s)$ with constant gain. Next $D(s) = d_0 + d_1 s$ was tried to get a positive real $h(s)$. In this case, with the suitable selection of coefficients d_0 and d_1, $h(s)$ can be made into a positive real transfer function. In order to implement $D(s) = d_0 + d_1 s$, a state variable filter after the induction machine output is required to provide filtered derivative of i_{df} as in Fig. 4.5.

In addition to these two conditions, the following conditions should be satisfied for stable identification, that is

$$\lim_{t \to \infty} \hat{a}_i(v,t) = a_i \quad and \quad \lim_{t \to \infty} \hat{b}_i(v,t) = b_i$$

- The machine to be identified is completely controllable.
- The components of the input are linearly independent.

Based on the above analysis, The implementation of identifier with a PI adaptation is shown in Fig. 4.7.

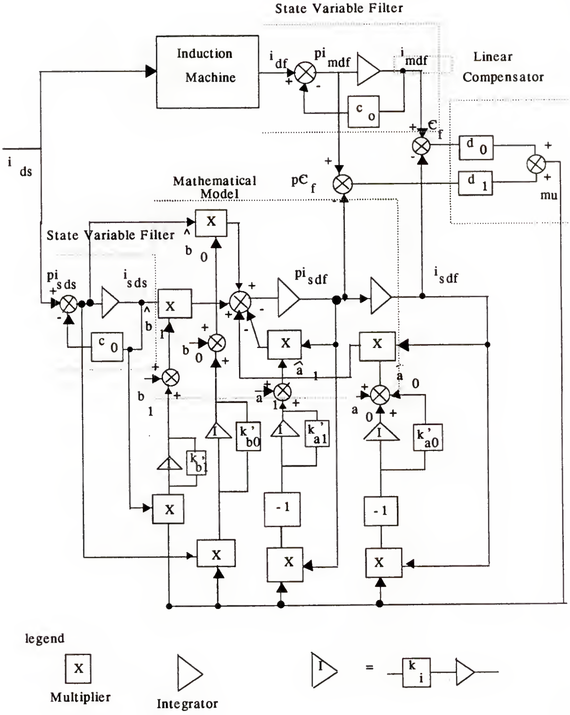

Fig. 4.7 Rotor resistance identifier with MRAS

CHAPTER 5

OPTIMAL EFFICIENCY CONTROL OF AN INDUCTION MACHINE

5.1 Analysis of Induction Machine Losses

The total induction machine loss consists of the following components:

(1) Copper loss (I^2R loss) — Copper loss depends on the effective resistance at the operating frequency and flux conditions. Stator copper loss is a function of torque, stator voltage and temperature. Rotor Copper loss is a function of torque, slip and temperature.

(2) Core loss — Core loss consists of the hysteresis and eddy current loss arising from changing flux density in the iron of the machine. Stator core loss is a function of stator voltage and frequency. Rotor core loss is a function of slip.

(3) Mechanical loss — Mechanical loss consists of friction and windage loss. This is mainly a function of speed.

(4) Stray loss — Stray loss consists of the losses arising from nonuniform current distribution in the copper and the additional losses produced in the iron by distortion of the magnetic flux by the load current. This is a function of stator voltage, frequency and temperature.

The above losses are represented by the resistances in the equivalent circuit of the induction machine shown in Fig. 5.1. For convenience, the following new impedances are defined:

$$z_1 = r_s + j\omega_e L_{ls} \qquad (5.1-1)$$

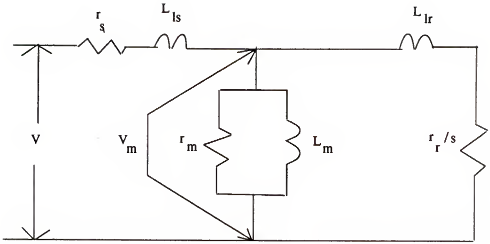

Fig. 5.1 Per phase equivalent circuit of an induction machine

$$z_2 = r_r \omega_e / \omega_s + j\omega_e L_{lr} \tag{5.1-2}$$

$$z_m = r_m j\omega_e L_m / (r_m + j\omega_e L_m) \tag{5.1-3}$$

$$z_T = z_1 z_2 + z_1 z_m + z_2 z_m \tag{5.1-4}$$

The core losses are usually modelled globally by a resistor connected in parallel with the magnetizing reactance. In order to represent the effects of frequency and harmonics, these losses must be separated into hysteresis and eddy current components. Each of these components is then divided into its stator and rotor contributions. The hysteresis losses are proportional to the frequency and eddy current losses are proportional to the square of the frequency. Rotor eddy current loss is proportional to the square of the slip frequency [16]. Based on these assumptions, the equivalent core loss resistor can be derived as follows. At supply frequency f, the stator core loss is

$$P_{cs} = \beta_h f \Phi^2 + \beta_e f^2 \Phi^2 \qquad (5.1-5)$$

where Φ is a air-gap flux and it is proportional to V_m/f, i.e.,

$$\Phi = \frac{V_m}{kf} \qquad (5.1-6)$$

and β_e and β_h are the hysteresis and eddy current coefficients, respectively, which will be explained later. The rotor core loss is

$$P_{cr} = \beta_h s f \Phi^2 + \beta_e s^2 f^2 \Phi^2 \qquad (5.1-7)$$

where s is slip. From the equivalent circuit shown in Fig. 5.1, total core loss is

$$P_{ct} = \frac{V_m^2}{r_m} = P_{cs} + P_{cr} \qquad (5.1-8)$$

Plugging (5.1–6) into (5.1–5) and (5.1–7) and from (5.1–8), we get

$$\frac{V_m^2}{r_m} = \left\{\beta_h \left(f + sf\right) + \beta_e \left(f^2 + s^2 f^2\right)\right\} \frac{V_m^2}{k^2 f^2} \qquad (5.1-9)$$

So the equivalent core loss resistor can be represented as follow:

$$r_m = \frac{r_{m_{nom}}}{\beta_h \left(1 + s\right)/f + \beta_e \left(1 + s^2\right)} \qquad (5.1-10)$$

β_h and β_e are, respectively, the per unit values of the hysteresis and eddy current losses in the stator for a 1.0 p.u. flux at rated frequency. Usually, only the sum of β_h and β_e is known, and an estimate of their ratio is thus needed: this ratio is difficult to measure, but an equipartition of the losses at 60 Hz is generally accepted as a reasonable assumption. Moreover, calculations have shown that substantial variations in this ratio have little impact on the results. This partition is assumed to be independent of the flux. The same principle and the same parameters β_h and β_e are used to calculate the core losses in the rotor. In this case, however, the rotor frequency replaces the source frequency [45].

5.2 Rotor Flux Selection for the Optimal Efficiency Control

The following problem is considered: For a given operating point defined by T_e (torque) and ω_r (speed), find the optimal rotor flux level which minimizes total machine loss (rotor copper loss, stator copper loss, core loss), assuming that the friction and windage loss is constant. The optimal rotor flux level will be used as an input command to the field oriented controller. The approach to the solution is to consider the slip as the independent variable and to search for the value of slip which minimizes the machine losses. The optimal rotor flux level is decided by the optimal slip.

When the machine is operating with field oriented control, the slip frequency can be represented by

$$\omega_s = \left(\frac{4}{3P}\right)\frac{T_e r_r}{\lambda_r^2} \qquad (5.2-1)$$

which may be derived from (3.2–2), (3.2–7) and (3.2–8). The source frequency is calculated as using the constraint on the speed. The source frequency is calculated as

$$f = \frac{\omega_s + \omega_r}{2\pi} \qquad (5.2-2)$$

The machine parameters in Fig. 5.1 are evaluated based on the source frequency and slip frequency. Core loss resistance r_m is calculated according to (5.1–10), and the impedances defined in (5.1–1)-(5.1–4) are also calculated. With these parameters, machine loss can be evaluated. The total machine loss is

$$P_t = |I_s|^2 r_s + |I_r|^2 r_r + |V_m|^2 / r_m \qquad (5.2-3)$$

With the defined impedances in (5.1–1)-(5.1–4), we can rewrite (5.2–3) as

$$P_t = V^2 \left\{ \left| \frac{z_2 + z_m}{z_T} \right|^2 r_s + \left| \frac{z_m}{z_T} \right|^2 r_r + \left| \frac{z_m z_2}{z_T} \right|^2 / r_m \right\} \qquad (5.2-4)$$

Since the speed is constant, only frequency and voltage can be varied to reduce the loss. The expression for the torque is from the equivalent circuit

$$T_e = \frac{3}{\omega_e} I_r^2 \frac{r_r}{s} = \frac{3}{\omega_s} \left| \frac{z_m}{z_T} \right|^2 V^2 r_r \qquad (5.2-5)$$

The expression for V^2 as a function of torque from (5.2–5) is

$$V^2 = \frac{T_e \omega_s}{3 r_r} \left| \frac{z_T}{z_m} \right|^2 \qquad (5.2-6)$$

Substituting (5.2–6) into (5.2–4) gives

$$P_t = \frac{T_e}{3 r_r} \left\{ \left| \frac{z_2 + z_m}{z_m} \right|^2 r_s + r_r + \frac{|z_2|^2}{r_m} \right\} \qquad (5.2-7)$$

Our problem is now reduced to following: Find the slip frequency ω_s, which minimizes (5.2–7). The optimal flux level will then be determined by (5.2–1) with the calculated optimal slip frequency. Analytical solution of the above problem is very difficult, because the impedance is itself a fuction of slip. A numerical method is used to solve the optimization problem and the algorithm is described in Fig. 5.2. In this flowchart, the nominal rotor flux value (λ_r) is determined from the given operating condition (i.e. rotor speed ω_r and torque T_e) may be derived from (5.2–1) as

$$\lambda_r^{nom} = \sqrt{\left(\frac{4}{3p}\right) \frac{T_e r_r}{(\omega_e - \omega_r)}} \qquad (5.2-8)$$

Minimization of the machine loss can be achieved by decreasing the rotor flux level. Results of the minimization (i.e. optimal rotor flux level) will be kept in a look-up table as a function of rotor speed, torque and rotor resistance for the implementation. Normally the optimal rotor flux selector starts after the torque and speed of the machine are in steady-state.

5.3 Theoretical Results

The core loss and the copper loss of a 60 Hz, 4–pole, 3 hp test induction machine are plotted in Fig. 5.3 and Fig. 5.4. for different slip frequencies. The machine parameters are given in the Appendix, and the rated speed is 1710 rpm.

As the rotor flux is decreased (i.e. slip frequency is increased), the copper losses for the given torque command are increased. But the core loss is decreased, as the slip frequency is increased. As shown in Fig. 5.4, the total machine loss has a minimum point. This point can be defined as an optimal slip frequency.

The optimization outlined in the previous section provides more efficient operation by controlling the level of rotor flux command in the field oriented controller. The following two aspects should be considered in designing the controller:

(1) The flux level should be varied with the torque command to keep an optimal balance between the core loss and the stator losses.

(2) The flux level should be varied with the speed, because the core losses increase with frequency. A higher flux level at low frequencies reduces the copper losses, while creating only a small increase in the core loss.

Fig. 5.5 and Fig. 5.6 show the optimal rotor flux level and slip frequency for different rotor speeds. As shown in Fig 5.6, if the saturation is neglected, the optimal slip frequency is independent of the torque command. This can be explained as follows. If the saturation is neglected, there is a unique value of slip frequency which is optimal for

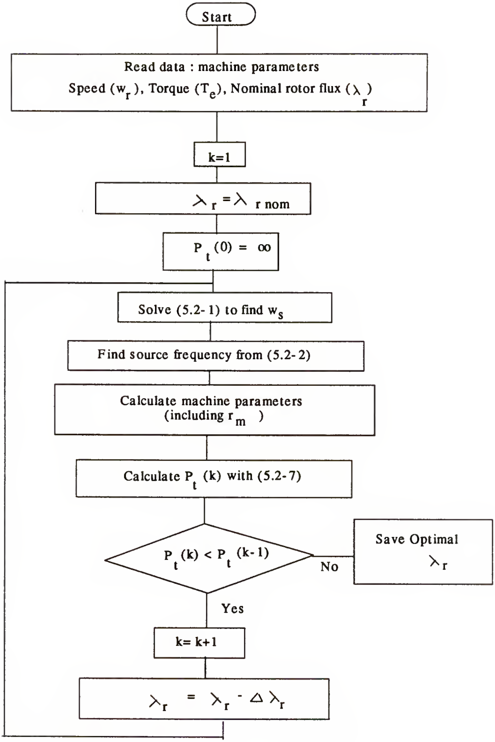
Start
Read data : machine parameters
Speed (w_r), Torque (T_e), Nominal rotor flux (λ_r)
k=1
$\lambda_r = \lambda_{r\,nom}$
$P_t(0) = \infty$
Solve (5.2-1) to find w_s
Find source frequency from (5.2-2)
Calculate machine parameters (including r_m)
Calculate $P_t(k)$ with (5.2-7)
$P_t(k) < P_t(k-1)$
No
Save Optimal λ_r
Yes
k= k+1
$\lambda_r = \lambda_r - \Delta\lambda_r$

Fig. 5.2 Flow chart to find optimal rotor flux

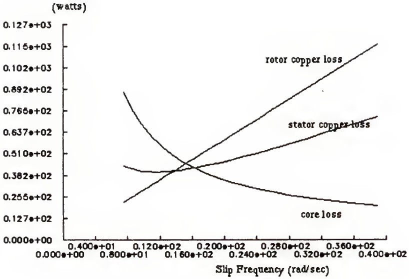

Fig. 5.3 Components of machine loss variation

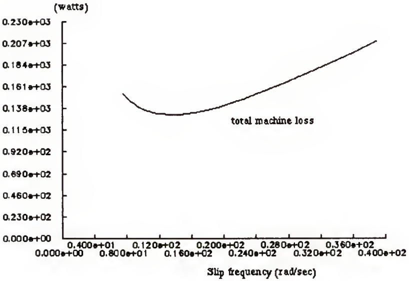

Fig. 5.4 Total machine loss variation

all load torques. Consider the equivalent circuit of the machine in Fig. 5.1 as a "source impedance" inserted between the stator voltage and a "load impedance" consisting of the apparent rotor resistance r_r/s. It is known from circuit theory, that a unique value of load impedance exists which results in the most efficient power transfer between the

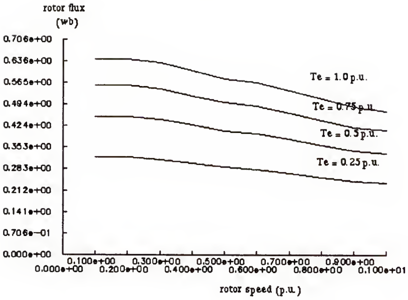

Fig. 5.5 Optimal rotor flux

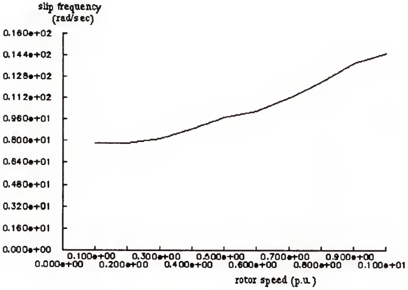

Fig. 5.6 Optimal slip frequency

source and load. This value is independent of the source voltage and thus of the amount of power transferred. Note in Fig. 5.6 the rotor speed is expressed in per unit of a base frequency of 1800 rpm, although the source (drive) frequency is still a variable determined in the optimization process.

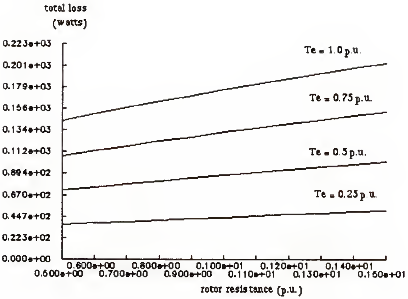

Fig. 5.7 Total machine loss for different rotor resistance

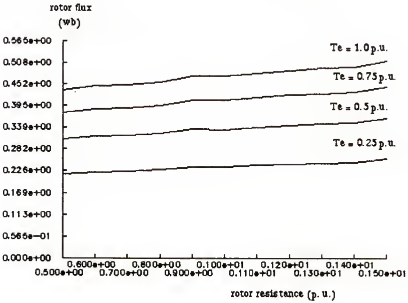

Fig. 5.8 Optimal rotor flux for different rotor resistance

As explained in Chapter 4, machine parameters are changing during operation. In order to calculate the optimal flux level, it is necessary to consider the change of machine parameters. Fig. 5.7 shows the total machine loss change for different rotor resistances. Fig. 5.8 shows the optimal flux level for different rotor resistance.

5.4 Proposed Optimal Efficiency Control

It is clear from the above analysis that induction machine loss can be minimized by controlling the rotor flux, for the given torque and speed commands. Moreover, a field oriented controller has the advantage of controlling the rotor flux directly. For the given torque and speed command, the optimal rotor flux level will be determined by the algorithm described in Section 5.2. The resulting torque and flux values will be used as input commands to the field oriented controller. The field oriented controller offers the following advantages for the optimal efficiency control:

(1) The rotor flux level is directly related to the combination of core loss and copper loss for the minimum machine loss, and it is available for the efficiency optimization.

(2) The torque or speed control loop can maintain the power output of the machine constant during optimization.

(3) The drive system can maintain satisfactory dynamic performance even when the machine is operating at reduced rotor flux.

It is established that machine loss is dependent on machine parameters which change with frequency and temperature. In order to calculate the optimal rotor flux level for the field oriented controller, precise information about the machine parameters is required. The most important machine parameter is rotor resistance, which can be identified by the method described in Chapter 4. The rotor resistance, which is the output of the identifier, should be considered in deciding the optimal rotor flux level for the given operating condition.

The overall block diagram of the new proposed optimal efficiency controller is shown in Fig. 5.9. The detailed field oriented controller can be found in Fig. 3.5, the rotor resistance identifier can be found in Fig 4.7, and the algorithm for finding the optimal

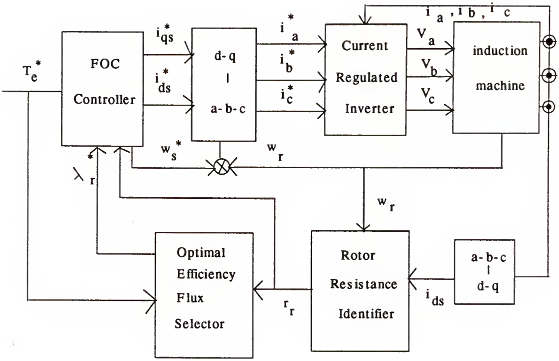

Fig. 5.9 Block diagram of optimal efficiency field oriented controller

rotor flux level is shown in Fig. 5.2. The proposed optimal efficiency controller has the following characteristics and advantages:

- The optimal rotor flux level is updated according to the output of the rotor resistance identifier.
- Accurate FOC can be achieved with the identified value of rotor resistance.
- The optimal rotor flux level can be selected directly from the given commands instead of changing rotor flux level gradually as in other method [17].
- This method requires no additional measurements over the standard indirect field oriented controller, in constrast to other optimizing techniques [17].

CHAPTER 6

SYSTEM SIMULATION

It is useful to simulate the operation of the new proposed optimal efficiency controller prior to its hardware implementation. The general purpose simulation program EMTP (Electro-Magnetic Transient Program) was used for this purpose. EMTP is comprised of four modules: the electric network (EN), the mechanical system (MS), the control system (TACS), and the universal machine (UM) module. The EN module allows simulation of various power system configurations, each with their own peculiar characteristics. The TACS module can be formulated in terms of block diagrams containing standard transfer functions and various special control devices. The MS module includes the entire electromechanical part of the machine. Actually it is represented as an electrical network after converting the mechanical system elements into their equivalent electric circuit elements. The UM module is the electromechanical energy conversion device which is connected to the EN and MS module. The interfacing of the above four modules constitutes the simulation of the induction machine drive system.

A 3 hp induction machine, whose parameters are given in the Appendix, is used as a test machine. In order to show the normal condition of operation, a speed controller as shown in Fig. 6.1 is simulated with EMTP. The optimal efficiency controller consists of four parts: the FOC controller, optimal efficiency flux selector, rotor resistance identifier and current regulated PWM inverter. The indirect field oriented controller as described in Fig. 3.5 is used for this drive, and is simulated with the TACS module.

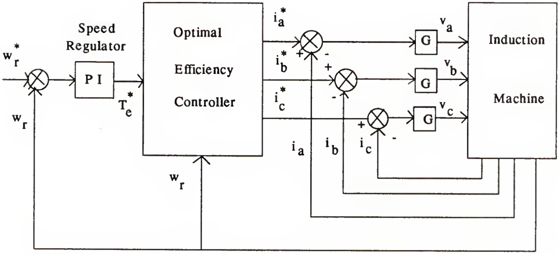

Fig. 6.1 Overall block diagram of simulated speed regulated drive system

6.1 Test of FOC Alone

In the first study, all the machine parameters of the test machine are assumed to be the nominal values which are used in the field oriented controller, and these parameters are assumed not to change during operation. Therefore a simulation of the rotor resistance identifier is unnecessary. The optimal rotor flux level also can be precalculated for a given operating condition, and this is the input command to the field oriented controller. The current regulated inverter is simulated as a variable voltage supply proportional to the current error between the actual and the reference current, as shown in Fig. 6.1. For the implementation of the FOC, a transformation from the $d-q$ axis to $a-b-c$ reference frame is required. This also can be simulated with TACS.

Fig 6.2 shows the transient torque response of the initial test system to a step change in the load torque, with a constant speed setting. Initially the machine was rotating at 184.73 rad/sec (0.98 p.u.), and at t = 0.1 sec. the load torque is changed from 4.44 Nm

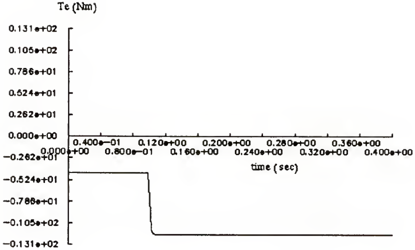

Fig. 6.2 Transient torque response to a step change in load torque

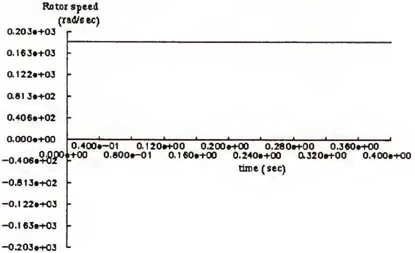

Fig. 6.3 Rotor speed characteristic for a step change in load torque

(0.37 p.u.) to 11.9 Nm (1.0 p.u.), and the rotor reference speed is held constant at 184.73 rad/sec (0.98 p.u.). In the EMTP simulation, when the machine is operated as a motor, electromagnetic torque has a negative value as shown in Fig. 6.2. Fig 6.3 shows the rotor speed response to the step change in load torque. Note the excellent performance obtained, without noticeable transients or oscillations relative to the speed command.

As explained in Chapter 4, parameters used in the field oriented controller must be accurate. In order to show the effects of using inaccurate parameters in the controller,

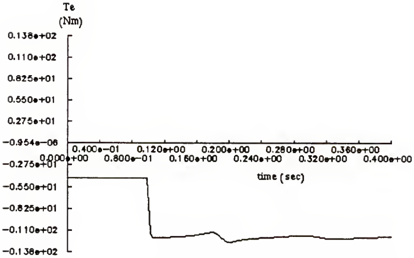

Fig. 6.4 Torque response with larger rotor resistance used in the controller

the overall system in Fig. 6.1 was simulated for two different cases. In this simulation, the machine was initially rotating at 184.73 rad/sec (0.98 p.u.). At t = 0.1 sec., the load torque is changed from 4.44 Nm (0.37 p.u.) to 11.9 Nm (1.0 p.u.) and the rotor reference speed is held at 184.73 rad/sec (0.98 p.u.). In Fig 6.4, the rotor resistance value used in the FOC controller is assumed to be 200 % of actual value. Fig. 6.4 shows undesirable oscillations in the electromagnetic torque for the change of load torque. Conversely in Fig. 6.5 the rotor resistance value used in the controller is assumed to be 20 % of actual value. In this case there is a slow convergence to the required load torque. These results agree with Fig. 4.4, i.e., a larger rotor time constant error causes the pole of the linearized transfer function between torque response and torque command current to be closer to the imaginary axis, and generally more poorly damped than for the correct FOC.

Next the effect of using an inaccurate rotor resistance value in the field oriented controller to a step change of the speed command is examined. The same 3–hp test machine whose parameters are given in the Appendix is also used in the simulation. Initially the induction machine was rotating at 184.73 (0.98 p.u.) with load torque 4.44 Nm (0.37 p.u.). At t = 0.1 sec., the rotor speed reference is changed to 94.25 rad/sec (0.5 p.u.) with same load torque. Three different cases are simulated. In Fig. 6.6, the

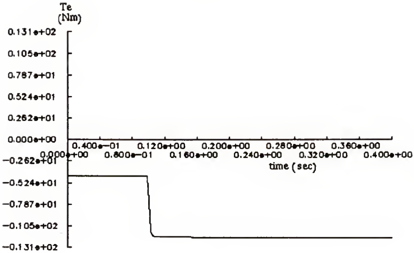

Fig. 6.5 Torque response with smaller rotor resistance used in the controller

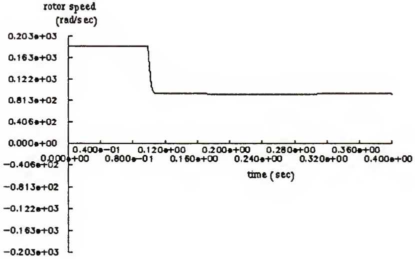

Fig. 6.6 Rotor speed response to a step change of the speed command with nominal rotor resistance

rotor reisistance used in the controller is assumed 100 % of nominal value. It shows the excellent speed change without transients.

In Fig. 6.7, for the same step change of speed command, the rotor resistance value used in the field oriented controller is assumed to be 200 % of the nominal value. There is an undesirable transient response after the step change of the speed command, and convergence to the given speed command is much slower than the speed response in Fig. 6.6.

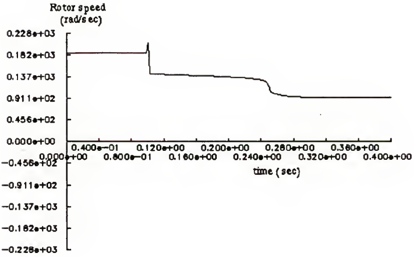

Fig. 6.7 Rotor speed response to a step change of the speed command with 200 % of the nominal rotor resistance

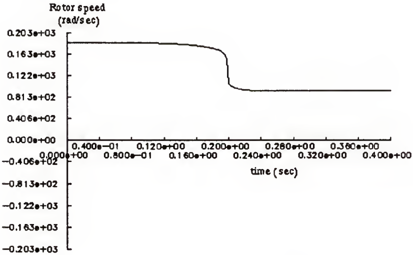

Fig. 6.8 Rotor speed response to a step change of the speed command with 20 % of the nominal rotor resistance

In Fig. 6.8, for the same step change of speed command, the rotor resistance value used in the field oriented controller is assumed to be 20 % of the nominal value. The convergence to the given speed command is also slower than in Fig. 6.6. Again it is shown that using inaccurate values of rotor resistance in the field oriented controller causes slower convergence to the speed command as was explained earlier in Sec. 4.1.

6.2 Test of the Rotor Resistance Identifier

For the operation of the correct FOC, the machine parameters (especially rotor resistance) used in the controller should be accurate values. Unfortunately during the normal operation of the drive, the value of the rotor resistance can change up to 200 % of nominal value as a function of the temperature [9]. In order to test the proposed control scheme, it is essential to change the rotor resistance of the tested machine and then estimate it. However, this method cannot be used directly in our simulation, since it is difficult to simulate a time varying rotor resistance in the EMTP universal machine module. Instead an approximation is used in the simulation, in which the induction machine is assumed to have a constant rotor resistance at the new value, while the measured stator currents and rotor speed (required as feedback signals in the control) are used to compute the magnetizing current from an assumed exponentially changing rotor resistance with a time constant of 0.06–0.6 sec. The necessary calculation is performed as shown below, which comes from (3.3–18)

$$i_{df} = \frac{r_r i_{qs}}{L_r\left(\omega_e - \omega_r\right)} \qquad (6.1-1)$$

A magnetizing current (i_{df}) can then be calculated. With the stator current (i_{ds}) and the magnetizing current (i_{df}), the rotor resistance can be estimated with the rotor resistance identifier, as indicated in the block diagram of Fig. 4.7. In the following study, the identified rotor resistance is compared with the actual rotor resistance, which is assumed to change exponentially.

In the simulation of the rotor resistance identifier, rotor resistance is assumed to change with load torque. The identified rotor resistance and actual rotor resistance for one case are shown in Fig. 6.9. In Fig. 6.9, the rotor resistance is assumed to change to 150 % of the nominal value exponentially with a time constant of 0.06 sec., following

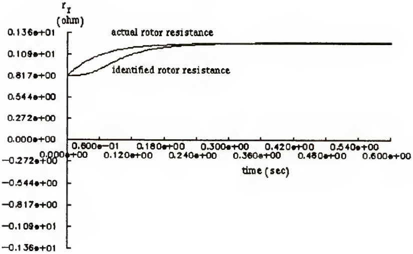

Fig. 6.9 The identified rotor resistance value a step change in load torque to 1.0 p.u.

a load torque change from 2.14 Nm (0.18 p.u.) to 11.9 Nm (1.0 p.u.). The identified rotor resistance tracks the actual rotor resistance without having a large overshoot or undershoot at the start of the identification, and converges to the actual value in about 0.24 sec. This characteristic is suitable for the application of the field oriented controller, which requires an accurate rotor resistance value.

In Fig. 6.10, the rotor resistance is assumed to change exponentially to 200 % of the nominal value, with a time constant of 0.06 sec., following a load torque change from 2.14 Nm (0.18 p.u.) to 17.85 Nm (1.5 p.u.). Similar response as in Fig. 6.9 is achieved, and the identified rotor resistance converges to the actual value in about 0.3 sec..

In Fig. 6.11, the rotor resistance is assumed to change exponentially to 200 % of the nominal value with a time constant of 0.6 sec., following a load torque change from 2.14 Nm (0.18 p.u.) to 17.85 Nm (1.5 p.u.). The time constant of the rotor resistance is increased to 0.6 sec., 10 times larger than the previous simulation. The identified rotor resistance shows a response as in Fig. 6.9 even for the larger time constant and the identified rotor resistance converges to the actual value in about 2.4 sec. For a slow change of rotor resistance, the identified rotor resistance has a larger overshoot during

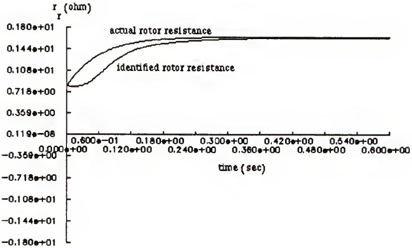

Fig. 6.10 The identified rotor resistance value for a step change in load torque to 1.5 p.u.

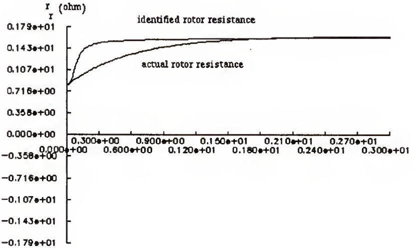

Fig. 6.11 The identified rotor resistance value for a step change in load torque to 1.5 p.u. with a slower change in rotor resistance

identification, which degrades the torque response compared to other cases. The main reason of this problem is that the coefficients of the rotor resistance identifier are tuned for the fast changing rotor resistance, therefore this problem can be solved by retuning the coefficients.

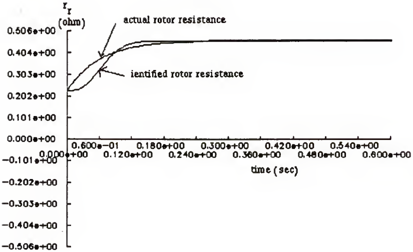

Fig. 6.12 The identified rotor resistance for a 50 hp induction machine for a step change in load torque to 1.0 p.u.

The proposed identifier was also applied to a 3–phase, 4–pole 50 hp induction machine whose parameters are also given in the Appendix. The actual rotor resistance is again assumed to change exponentially to 200 % of nominal value with time constant of 0.06 sec., following a change in load torque from 90.5 Nm (0.47 p.u.) to 190 Nm (1.0 p.u.). Fig. 6.12 shows the identified rotor resistance and actual rotor resistance for this case. The proposed identifier shows a similar characteristic as in the Fig. 6.9, with this larger induction machine.

The identified steady state values versus the actual rotor resistances of the 3 hp test machine are shown in Fig. 6.13. Robustness of the identifier will be discussed in section 6.4.

6.3 Full System Tests

As dicussed earlier, the complete optimal efficiency field oriented controller as shown in Fig. 6.1 is simulated with EMTP. A more detailed block diagram of the optimal efficiency controller can be found in Fig. 5.9. The rotor resistance identifier, whose block diagram is shown in Fig. 4.7, is also included in the simulation. In the simulation,

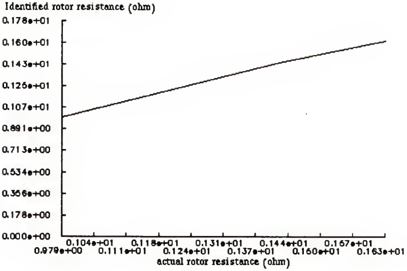

Fig. 6.13 Actual versus indentified rotor resistance for 3 hp test machine

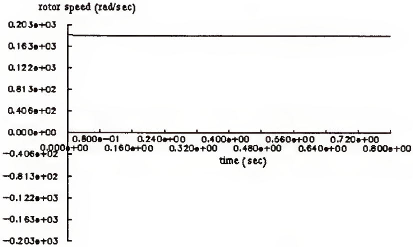

Fig. 6.14 Speed characteristic for a step change of load torque with rotor resistance identifier

the optimal rotor flux is determined by table look-up of precalculated values from the given torque and speed command, and the estimated rotor resistance. The 3 hp induction machine described in earlier tests is used in the complete simulation. In the results shown, the machine is initially rotating at 184.73 rad/sec (0.98 p.u.), and at t = 0.0 sec the load torque is changed from 2.26 Nm (0.18 p.u.) to 17.85 Nm (1.5 p.u.), and the rotor reference speed is held constant at 184.73 rad/sec (0.98 p.u.). The rotor resistance

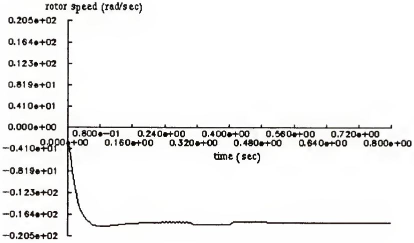

Fig. 6.15 The electromagnetic torque response to a step change in load torque with rotor resistance identifier operating

is assumed to change exponentially to 200 % of the nominal value with time constant of 0.06 sec. The optimal rotor flux selector starts working at 0.3 sec., when electromagnetic torque, rotor speed and identified rotor resistance are in steady-state. The rotor flux level, which is the input to the field oriented controller, is ramped from 0.8025 wb to the optimal value of 0.6582 wb in 0.1 sec. This simulates the time delay in calculating the rotor flux. The rotor speed response for the step change in the load torque is shown in Fig. 6.14. This shows that change of the rotor flux level hardly affects the constant rotor speed. The torque response of the induction machine to the step change in load torque, is shown in Fig. 6.15. Both figures show that the proposed identifier can be used with the field oriented controller which requires accurate rotor resistance value, because during the identification process the identified rotor resistance changes about 20 % of the actual value and converges to the actual value. Fig. 6.16 compares the actual rotor flux level with the rotor flux command.

The above load torque change at constant speed operation was also simulated without the rotor resistance identifier. The 3 hp test machine with the same operating condition was simulated. In this case the rotor resistance identifier is not used in the field oriented

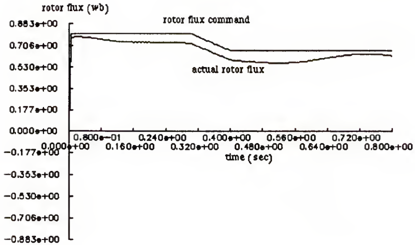

Fig. 6.16 Comparison of rotor flux and rotor flux command for a step change in load torque

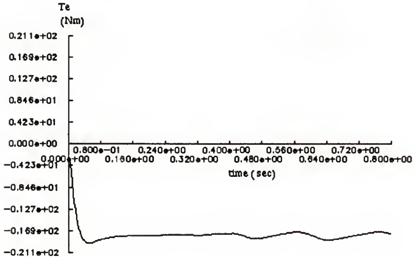

Fig. 6.17 Electromagnetic torque response to a step change in load torque without rotor resistance identifier

controller, but instead the rotor resistance is assumed to be 300 % of the nominal value, even though it actually changes to 200 % of the nominal value with a time constant of 0.06 sec. The electromagnetic torque for the step change in the load torque is shown in Fig. 6.17. This result shows without the rotor resistance identifier the torque response has a larger overshoot and convergence to the new load torque is slower than the torque response with the identifier.

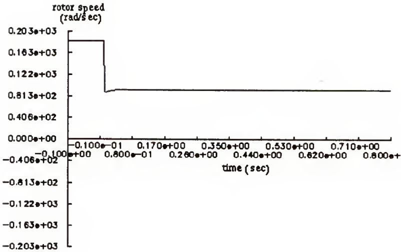

Fig. 6.18 The rotor speed response to a step change in speed command for the 50 hp induction machine with rotor resistance identifier

For a constant load torque, a change of speed command for the 50 hp induction machine was also simulated. The machine is initially rotating at 184.73 rad/sec (0.98 p.u.), and at t = 0 sec., the rotor speed command changes to 94.25 rad/sec (0.5 p.u.) with a load torque of 90 .5 Nm (0.47 p.u.). The optimal rotor flux selector starts working at 0.4 sec., when the the electromagnetic torque, the rotor speed and identified rotor resistance are in steady-state. The rotor flux level, which is the input to the field oriented controller, is ramped from 0.1057 wb to the optimal value of 0.1465 wb in 0.1 sec., to simulate the time delay in calculating of the rotor flux. In this simulation the rotor resistance is assumed to change exponentially to 200 % with time constant of 0.06 sec.. The rotor speed response with the rotor resistance identifier is shown in Fig. 6.18. Fig. 6.19 compares the actual rotor flux level with the rotor flux command.

The same operating conditon without the rotor resistance identifier is also simulated. The rotor resistance used in the controller is assumed to be the 250 % of the nominal value. The rotor speed response to the step change in speed command is shown in Fig. 6.20. By comparing Fig. 6.18 and Fig. 6.20, it is clear that the rotor resistance

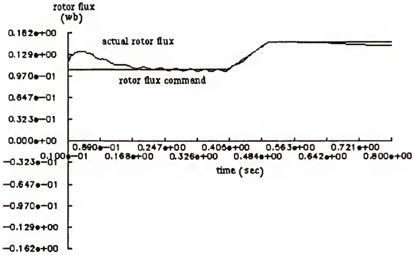

Fig. 6.19 Comparison of rotor flux and rotor flux command for a step change in speed command

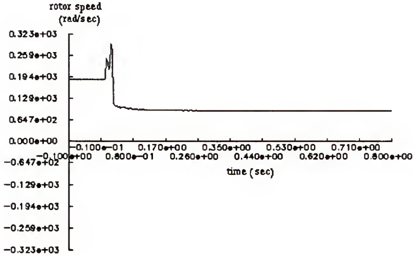

Fig. 6.20 The rotor speed response to a step change in speed command for the 50 hp induction machine without rotor resistance identifier

identifier improves the transient response produced by the FOC. This is a very important characteristic for high performance operation.

The optimal efficiency operation of the induction machine can be verified by measuring the input power to the induction machine for a given operating condition, i.e. load torque and speed command. The input power to the machine for different rotor

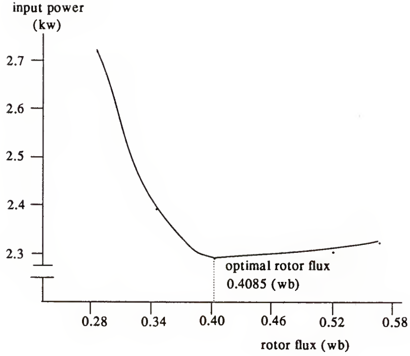

Fig. 6.21 Input power to the 3 hp induction machine for different rotor fluxes

flux commands is shown in Fig. 6.21 for the 3 hp induction machine. The machine is rotaing at 184.72 (0.98 p.u.) with a load torque of 8.925 Nm (0.75 p.u.). The optimal rotor flux value, which is calculated according to the flowchart in Fig. 5.2, is 0.4085 wb (0.72 p.u.). The value determined by the optimal flux selector therefore agrees with the minimum shown in Fig. 6.21.

The input power to the 50 hp induction machine for different rotor flux commands is shown in Fig. 6.22. The machine is rotating at 179.075 (0.95 p.u.) with a load torque of 190 Nm (1.0 p.u.). The optimal rotor flux value, which is calculated according to the flowchart in Fig. 5.2, is 1.2714 wb (0.9 p.u.). Fig. 6.22 again shows that the proposed optimal rotor flux selector generates the rotor flux value which gives an optimal efficiency. By using this optimal rotor flux value as an input command to the field oriented controller, optimal efficiency operation of the induction machine can be achieved.

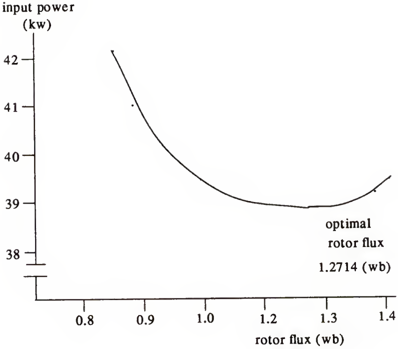

Fig. 6.22 Input power to the 50 hp induction machine for different rotor fluxes

6.4 Overall Controller Characteristics

Most of the previous rotor resistance identification methods are concerned with the steady-state rotor resistance. With Sugimoto's method [13], identification starts with a nominal value and takes about 2 seconds. With Kubota's method [42], the rotor resistance was identified when the measured variables were nearly constants. For use with change of speed or torque command, rotor resistance identification typically starts before the change of command is applied in order to get steady-state rotor resistance. Identification terminates in about 1.2 seconds. With Garces' method [9], identification terminates in 10 seconds. With Matuso's method [33], rotor resistance identification takes about 3 seconds. With Dalal's method [35], the step change compensation takes about 0.75 seconds to reach steady-state. The proposed identification method takes about 0.24 seconds for a fast change of the rotor resistance and it takes about 2.4 seconds for a slow change of the rotor resistance. For optimal efficiency operation with Kirchen's method [17], final

Table 6.1 Torque characteristics for different step change in load torques for 3 hp machine

Torque (p.u.)	Maximum % overshoot of torque	Response time to load torque (sec)	Rotor resistance identification error (%)
0.5	0.3	0.13	1.88
1.0	0.6	0.14	1.96
1.5	0.9	0.14	1.67
2.0	1.4	0.15	1.19

conditions are achieved in about 30 seconds. The proposed optimization method takes about 0.8 second to reach the optimal efficiency operation final conditions.

The proposed controller was tested at various operating conditions. The machine is initially rotating at 184.73 rad/sec (0.98 p.u.) with load torque of 2.14 Nm (0.18 p.u.) and rotor resistance changes to 200 % of the nominal value with a time constant of 0.06 sec. For a constant speed (184.73 rad/sec: 0.98 p.u.) operation of the 3-hp test machine, the torque response to the different commands is shown in Table 6.1. Table 6.1 shows that maximum percent overshoot of torque is within 1.5 % and response time to the torque command is less then 0.15 sec, while identified rotor resistance error is less than 2 %. This shows that the proposed controller works well with different load torque changes. It also shows that same identifier can be used with the different load torque without tuning the identifier.

For a constant load torque, the speed characteristics for a change of speed command are shown in Table 6.2. Machine is initially rotating at 184.73 rad/sec (0.98 p.u.) with load torque of 2.14 Nm (0.18 p.u.) and rotor resistance changes to 200 % of the nominal

Table 6.2 Speed characteritics for different step change in speed commands for 3 hp machine

Speed command (p.u.)	Response time to speed command (sec)	Rotor resistance identification error (%)
0.75	0.023	4.16
0.5	0.032	12.0
0.25	0.034	39.7

value with a time constant of 0.06 sec.. Table 6.2 shows that for the change in the speed command, the response time (with no overshoot) is less than 0.04 seconds, regardless of speed command. It also shows that tuning of the identifier is required for the large changes in speed command. Therefore, the coefficients in the rotor resistance identifier should be changed for a large step change of the speed command.

The torque characteristics for a constant speed (184.73 rad/sec: 0.98 p.u.) operation with a change in load torque command from 2.14 Nm (0.18 p.u.) to 11.9 Nm (1.0 p.u.) for different rotor resistance characteristic is shown in Table 6.3. In this table rotor resistance changes to 120 %,150 %, 175 % and 200 %, respectively, with a time constant of 0.06 sec. It shows that as the rotor resistance increases, the maximum percent overshoot increases but response time decreases. Therefore, it is shown that the same identifier works well for different rotor resistance.

The speed charateristics for different rotor resistance characteristics with same load torque (2.14 Nm: 0.18 p.u.) and same step change of speed command from (184.73 rad/sec : 0.98 p.u.) to (94.25 rad/sec: 0.5 p.u.) is shown in Table 6.4. In this table rotor resistance changes to 120 %,150 %, 175 % and 200 %, respectively, with a time constant of 0.06 sec. Response time to speed command increases and identification error

Table 6.3 Torque change characteristics for different rotor resistance characteristics in 3 hp machine

Rotor resistance (p.u.)	maximum % overshoot of torque	Response time to torque command (sec)	Rotor resistance identification error (%)
1.2	no	0.2	0.7
1.5	0.22	0.14	0.5
1.75	1.43	0.14	1.9
2.0	1.63	0.14	1.9

Table 6.4 Speed change characteristics for different rotor resistance characteristics in 3 hp machine

Rotor resistance (p.u.)	Response time to speed command (sec)	Rotor resistance identification error (%)
1.2	0.065	16.4
1.5	0.051	15.9
1.75	0.051	11.4
2.0	0.032	11.2

decreases as the rotor resistance increases, therefore, identifier may require tuning for these speed change operations.

The torque characteristics for different machines, with the same change in torque command from 0.18 p.u. to 1.0 p.u. with the same rotor speed (0.98 p.u.) is shown in Table 6.5. The rotor resistance identifer needs to be tuned for the different machines.

Table 6.5 Torque characteristics for different step change in load torques for 3 hp machine

Machine rating	Maximum % overshoot of torque	Response time to torque command (sec)	Rotor resistance identification error (%)
3 hp	0.6	0.14	1.96
50 hp	11.6	0.46	2.0
500 hp	19.2	0.56	9.4

Table 6.6 Energy savings for different machines

Machine rating	Input power without optimal efficiency controller (kw)	Input power with optimal efficiency controller (kw)	% Input power saving
3 hp	2.321	2.278	1.9
50 hp	39.263	38.805	1.2

Energy savings with the optimal efficiency controller based on Fig. 6.21 and 6.22 are shown in Table 6.6. The 3 hp machine is rotaing at 184.73 (0.98 p.u.) with a load torque of 8.925 Nm (0.75 p.u.). The optimal rotor flux value, which is calculated according to the flowchart in Fig. 5.2, is 0.4085 wb (0.72 p.u.). The 50 hp machine is rotating at 179.075 (0.95 p.u.) with a load torque of 190 Nm (1.0 p.u.). The optimal rotor flux value, which is calculated according to the flowchart in Fig. 5.2, is 1.2714 wb (0.9 p.u.).

CHAPTER 7

SUMMMARY AND CONCLUSIONS

This dissertation has investigated a new optimal efficiency control scheme of an induction machine. It is known that the efficiency of the induction machine can be improved by controlling the flux level in the machine. The control of the flux can be achieved with a field oriented controller. The main idea of the field oriented control is that the induction machine can be controlled like a separately excited dc machine, by adjusting the stator current as a vector quantity with a torque and flux component. By employing a similar control strategy of the dc machine, excellent transient reponse can be achieved with field oriented control. One of the advantages of the field oriented control is that it provides a direct access to the flux level in the machine. For the implementation of the field oriented controller, stator currents should be controlled instantaneously. This can be realized with a current regulated pulse-width modulated (CRPWM) inverter.

The widely used indirect field oriented control method was used in this investigation. In this type of field oriented controller, the angular position of the rotor flux is indirectly estimated or measured based on the rotor speed and rotor time constant. The main disadvantage of the indirect method is that the value of rotor resistance used in the controller must be accurate. Unfortunately the rotor resistance changes with temperature during operation. Therefore the rotor resistance used in the controller is estimated by a rotor resistance identifier, which utilizes single-input-single-output (SISO) model reference adaptive system (MRAS). Since the same measured stator currents and rotor speed, which are required in the indirect field oriented controller itself, are also needed in the identifier, no additional measurement is needed. The structure of the identifier is also simpler than the existing methods. In addition, since the identifier is based on the dynamic equations of the induction machine, transient variation of the rotor resistance can be identified.

With the identified rotor resistance for a given operating condition, the optimal efficiency rotor flux is calculated based on an equivalent circuit, which includes frequency dependent core loss resistance and the identified rotor resistance. The optimal rotor flux level is used as an input command to the field oriented controller.

In order to show the validity of the proposed system, a speed regulator with rotor resistance identifier and optimal rotor flux selector, is simulated using the Electro-Magnetic Transient Program (EMTP). The simulation results show excellent speed characteristic without transients by using the rotor resistance identifier. The optimal efficiency operation of the machine is verified by measuring the input power to the induction machine for a given operating condition.

The proposed optimal efficiency field oreinted controller has following advantages:

- Accurate field oriented control is achieved by updating the parameters used in the controller with the rotor resistance identifier.
- The rotor resistance identifier needs only stator currents and rotor speed measurements, therefore no additional measurements are needed over that required for the indirect FOC.
- Since the proposed rotor resistance identifier is based on a single-input-single-output (SISO) model reference adaptive system (MRAS), the structure of the identifier is simpler than existing methods.
- Since the optimal flux level is dependent on the variation of rotor resistance, a more accurate rotor flux level can be calculated.
- The convergence to the optimal efficiency point is faster than the existing methods.

Further research is recommended in the following areas:

- Testing of the proposed system with experiment.
- Controller design with consideration of machine saturation

APPENDIX

Details of 3 hp Test Machine

Nameplate data:

squirrel-cage induction machine;

3 hp, 230 V, 5.8 A;

1710 rpm, 60 Hz, three-phase, four poles.

Parameter values;

base impedance = 21.62 Ω

stator resistance r_s = 0.435 Ω (0.0201 p.u.)

rotor resistance r_r = 0.816 Ω (0.0377 p.u.)

stator leakage reactance X_{ls} = 0.754 Ω (0.0349 p.u.)

rotor leakage reactance X_{lr} = 0.754 Ω (0.0349 p.u.)

magnetizing reactance X_m = 26.13 Ω (1.2082 p.u.)

inertia of the rotor J = 0.089 (kg.m^2)

inertia constant H = 0.7065 (s)

Details of 50 hp Test Machine

Nameplate data:

squirrel-cage induction machine;

50 hp, 460 V, 46.8 A;

1705 rpm, 60 Hz, three-phase, four poles.

Parameter values;

base impedance = 5.6729 Ω

stator resistance r_s = 0.087 Ω (0.0153 p.u.)

rotor resistance r_r = 0..228 Ω (0.0402 p.u.)

stator leakage reactance X_{ls} = 0.302 Ω (0.0532 p.u.)

rotor leakage reactance X_{lr} = 0.302 Ω (0.0532 p.u.)

magnetizing reactance X_m = 13.04 Ω (2.2986 p.u.)

inertia of the rotor J = 1.662 (kg.m^2)

inertia constant H = 0.7916 (s)

Details of 500 hp Test Machine

Nameplate data:

squirrel-cage induction machine;

500 hp, 2300 V, 93.6 A;

1773 rpm, 60 Hz, three-phase, four poles.

Parameter values;

base impedance = 14.1823 Ω

stator resistance r_s = 0.262 Ω (0.0185 p.u.)

rotor resistance r_r = 0.187 Ω (0.0132 p.u.)

stator leakage reactance X_{ls} = 1.206Ω (0.0850 p.u.)

rotor leakage reactance X_{lr} = 1.206 Ω (0.0850 p.u.)

magnetizing reactance X_m = 54.02 Ω (3.8090 p.u.)

inertia of the rotor J = 11.06 (kg.m^2)

inertia constant H = 0.5268 (s)

REFERENCES

[1] F. Blaschke, "The Principle of Field Orientation as Applied to the New Trans-Vector Closed-Loop Control System for Rotating Field Machines," Simens Review, vol. 34, pp. 217–220, 1972.

[2] P. Krause and C. H. Thomas, "Simulation of Symmetrical Induction Machinery," IEEE Transaction on Power Apparatus and Systems., vol. PAS-84, pp. 1038–1053, 1965.

[3] P. Krause, "Analysis of Electric Machinery," McGraw-Hill Inc., New York, 1986.

[4] K. Hirose, A. Kawamura and R. Hoft, "Comparison of Field Oriented and Field Acceleration Methods of Induction Motor Control," IEEE Power Electronics Specialist Conference Record, pp. 91–101, 1984.

[5] G. Gabriel, W. Leonhard and C. Nordby, "Field Oriented Control of Standard AC motor Using Microprocessors," IEEE Transaction on Industry Applications, vol. IA-16, pp. 186–192, 1980.

[6] W. Leonhard, "Control of Electrical Drives," Springer-Verlag, Berlin, Heidelberg, 1985.

[7] A. Nabae, K. Otsuka, H. Uchino and R. Kurosawa, "An Approach to Flux Control of Induction Motors Operated with Variable-Frequency Power Supply," IEEE Transaction on Industry Applications, vol. IA-16, pp.342–350, 1980.

[8] K. Nordin, D. Novotny and D. Zinger, "The Influence of Motor Parameter Deviations in Feedforward Field Orientation Drive Systems," IEEE Transaction on Industry Applications, vol. IA-21, pp. 1009–1015, 1985.

[9] L. Garces, "Parameter Adaptation for the Speed-Controlled Static AC Drive with a Squirrel-Cage Induction Motor," IEEE Transaction on Industry Applications, vol. IA-16, pp. 173–178, 1980.

[10] M. Koyama, M. Yano, I. Kamiyama and S. Yano, "Microprocessor-Based Vector Control System for Induction Motor Drives with Rotor time Constant Identification Function," IEEE IAS Annual Meeting Conference Record, pp. 564–569, 1985.

[11] T. Ohtani, "A New Method of Torque Control Free From Motor Parameter Variation in Induction Motor Drives," IEEE IAS Annual Meeting Conference Record, pp. 203–209, 1986.

[12] Y. Landau, "Adaptive Control – The Model Reference Approach," Marcel Dekker Inc., New York, 1979.

[13] H. Sugimoto and S. Tamai, "Secondary Resistance Identification of an Induction Motor Applied Model Refernce Adaptive System and its Characteristics," IEEE IAS Annual Meeting Conference Record, pp. 613–620 1985.

[14] K. Ohnishi, Y. Ueda and K. Miyachi, "Model Reference Adaptive System against Rotor Resistance Variation in Induction Motor Drive," IEEE Transaction on Industrial Electronics, vol. IE-33, pp. 217–223, 1986.

[15] A. Kusko and D. Galler, "Control Means for Minimization of Losses in AC and DC Motor Drives," IEEE Transaction on Industry Applications, vol. IA-19, pp. 561–570, 1983.

[16] H. G. Kim, S. K. Sul and M. H. Park, "Optimal Efficiency Drive of a Current Source Inverter Fed Induction Motor by Flux Control," IEEE Transaction on Industry Applications, vol. IA-20, 1984.

[17] D. W. Kirchen, D. W. Novotny and T. Lipo, "Optimal Efficiency Control of an Induction Motor Drive," IEEE Transaction on Energy Conversion, vol. EC-2, pp. 70–76, 1987.

[18] B. K. Bose, "Adjustable Speed AC Drives- A Technology Status Review," Proceedings of the IEEE, vol. 60, pp. 116–135, 1982.

[19] T. Ito, T. Yamaguchi, R. Ueda, T. Mochizuki and S. Takata, "Analysis of Field Orientation Control of Current Source Inverter Drive Induction Motor Systems," IEEE Transaction on Industry Applications, vol. IA-19, pp. 206–210, 1983.

[20] S. Sathikumar and J. Vithayathil, "Digital Simulation of Field Oriented Control of Induction Motor," IEEE Transaction on Industrial Electronics, vol. IE-31, pp. 141–148, 1984.

[21] S. Yamamura, "AC Motors for High-Performance Applications: Analysis and Control," Marcel Dekker Inc., New York, 1986.

[22] F. Alashhab, R. Hoft and A. Kawamura, "Matrix Transformation Analysis to Derive Unique Features of FOC and FAM Induction Motor Control," IEEE IAS Annual Meeting Conference Record, pp. 586–600, 1985.

[23] B. K. Bose, "Power Electronics and AC Drives," Prentice-Hall, Englewood Cliffs, New Jersey, 1986.

[24] T. M. Rowan and R. J. Kerkman, "A New Synchronous Current Regulator and Analysis of Current Regulated PWM Inverters," IEEE IAS Annual Meeting Conference Record, pp. 487–495, 1985.

[25] R. D. Lorenz, M. O. Lucas and D. B. Lawson, "Performance of Feed Forward Current Regulators for Field Oriented Induction Machine Controllers," IEEE IAS Annual Meeting Conference Record, pp. 99–105, 1986.

[26] R. D. Lorenz and D. M. Divan, "Dynamic Analysis & Experimental Evaluation of Delta Modulators for Field Oriented AC machine Current Regulators," IEEE IAS Annual Meeting Conference Record, pp. 196–210, 1987.

[27] P. Enjeti, P. D. Ziogas, J. F. Lindsay and M. H. Rashid, "A New Current Control Scheme for AC Motor Drives," IEEE IAS Annual Meeting Conference Record, pp. 202–208, 1987.

[28] R. Krishnan and P. Pillay, "Sensitivity Analysis and Comparison of Parameter Compensation Scheme in Vector Controlled Induction Motor Drives," IEEE IAS Annual Meeeting Conference Record, pp. 147–154, 1986.

[29] H. Nagase, Y. Matsuda, K. Ohnishi, H. Ninomiya and T. Koike, "High-Performanc Induction Motor Drive System Using a PWM Inverter," IEEE Transaction on Industry Application, vol. IA-20, pp. 1482–1489, 1984.

[30] T. Irisa, S. Takata, R. Ueda, T. Sonoda and T. Mochizuki, "A Novel Approach on a Parameter Self-Tuning Method in AC Servo System," Automatica, pp. 287–294, 1986.

[31] S. Sivakumar, A. M. Sharaf and K. Natarajan, "Improving the Performance of Indirect Field Oreintation for Induction Motor Drives," IEEE IAS Annual Meeting Conference Record, pp. 147–154, 1986.

[32] R. D. Lorenz, "Tuning of Field Oriented Induction Motor Controllers for High Performance Applications," IEEE IAS Annual Meeting Conference Record, pp. 607–612, 1985.

[33] T. Matsuo and T. Lipo, "A Rotor Parameter Identification Scheme for Vector-Controlled Induction Motor Drives," IEEE Transaction on Industry Applications, vol. IA-21, pp. 624–632, 1985.

[34] S. K. Sul, "A Novel Technique of Rotor Resistance Estimation Considering Variation of Mutual Inductance," IEEE IAS Annual Meeting Conference Record, pp. 184–188, 1987.

[35] D. Dalal and R. Krishnan, "Parameter Compensation of Indirect Vector Controlled Induction Motor Drive Using Estimated Airgap Power," IEEE IAS Annual Meeting, Conference Record, pp. 170–176, 1987.

[36] R. D. Lorenz and D. B. Lawson, "Flux and Torque Decoupling Control for Field Weakened Operation of Field Oriented Induction Machines," IEEE IAS Annual Meeting Conference Record, pp. 132–137, 1987.

[37] W. Deleroi, A. Fahim and J. B. Woudstra, "Parameters Adaptation for Transient Operation of Three Phase Squirrel Cage Induction Mortor," IEEE IAS Annual Meeting Conference Record, pp. 63–68, 1987.

[38] C. Wang, D. W. Novotny and T. A. Lipo, "An Automated Rotor Time Constant Measurement System for Indirect Field Oriented Drives," IEEE Transaction on Industry Applications, vol. IA-24, pp. 151–159, 1988.

[39] A. Kumamoto, S. Tada and Y. Hirane, "Optimal Speed Regulator of a Transvector-Controlled Induction Motor Drive System Using a Model Reference Adaptive System," IEEE Industial Electronics Conference Record, pp. 195–200, 1985.

[40] S. Tamai, H. Sugimoto and M. Yano, "Speed Sensor-Less Vector Control of Induction Motor with Model reference Adaptive System," IEEE IAS Annual Meeting Conference Record, pp. 189–195, 1987.

[41] L. C. Zai and T. A. Lipo, "An Extended Kalman Filter Approach to Rotor Time Constant Measurement in PWM Induction Motor Drives," IEEE IAS Annual Meeting Conference Record, pp. 177–183, 1987.

[42] H. Kubota, K. Matsuse and T. Fukao, "New Control Method of Inverter-Fed Induction Motor Drive by Using State Observer with Rotor Resistance Identification," IEEE IAS Annual Meeting, Conference Record, pp. 601–606, 1985.

[43] N. Mohan, "Improvement in Energy Efficiency of Induction Motors by means of Voltage Control," IEEE Transaction on Power Apparatus and Systems, vol. PAS-99, 1466–1471, 1980.

[44] T. W. Jian, N. L. Schmitz and D. W. Novotny, "Charateristic Induction Motor Slip Values for Variable Voltage Part Load Performance Optimization," IEEE Transaction on Power Apparatus and Systems, vol. PAS-102, pp. 38–46, 1983.

[45] D. S. Krischen, D. W. Novotny and W. Suwanwisoot, "Minimizing Induction Motor Losses by Excitation Control in Variable Frequency Drives," IEEE Transaction on Industry Applications, vol. IA-20, pp. 1244–1250, 1984.

[46] I. Takahashi and T. Noguchi, "A New Quick-Response and High-Efficiency Control Strategy of an Induction Motor," IEEE Transaction on Industry Application, vol. IA-22, pp. 820–827, 1986.

[47] W. S. Meyer and T. H. Liu, Eds., "EMTP Rule Book," Portland, Oregon: Bonneville Power Administration, System Engineering, Jun. 1984.

[48] Z. Daboussi and N. Mohan, "Digital Simulation of Field-Oreinted Control of Induction motor Drives Using EMTP," 1988 IEEE/PES Winter Meeting Record.

[49] D. M. Brod and D. W. Novotny, "Current Control of VSI-PWM Inverters," IEEE Transaction on Industry Application, vol. IA-21, pp. 562–570, 1985.

BIOGRAPHICAL SKETCH

Sung Chul Oh was born on January 23, 1958 in Jinhae, Korea. He recieved the B.S. and M.S. degrees in electrical engineering form Seoul National University, Seoul, Korea, in 1980 and 1982, respectively. From 1982 to 1983 he worked as a research engineer for the Korea Electrotechnology Research Institute.

I certify that I have read this study and that in my opinion it conforms to acceptable standards of scholarly presentation and is fully adequate, in scope and quality, as a dissertation for the degree of Doctor of Philosophy.

DP Carroll

Dr. D. P. Carroll, Chairman
Professor of Electrical Engineering

I certify that I have read this study and that in my opinion it conforms to acceptable standards of scholarly presentation and is fully adequate, in scope and quality, as a dissertation for the degree of Doctor of Philosophy.

Dr. R. L. Sullivan
Professor of Electrical Engineering

I certify that I have read this study and that in my opinion it conforms to acceptable standards of scholarly presentation and is fully adequate, in scope and quality, as a dissertation for the degree of Doctor of Philosophy.

Giuseppe Basile

Dr. G. Basile
Professor of Electrical Engineering

I certify that I have read this study and that in my opinion it conforms to acceptable standards of scholarly presentation and is fully adequate, in scope and quality, as a dissertation for the degree of Doctor of Philosophy.

Alex Domijan, Jr

Dr. A. Domijan, Jr.
Assistant Professor of Electrical Engineering

I certify that I have read this study and that in my opinion it conforms to acceptable standards of scholarly presentation and is fully adequate, in scope and quality, as a dissertation for the degree of Doctor of Philosophy.

Barney L Capehart

Dr. B. L. Capehart
Professor of Industrial and Systems
Engineering

This dissertation was submitted to the Graduate Faculty of the College of Engineering and to the Graduate School and was accepted as partial fulfillment of the requirements for the degree of Doctor of Philosophy.

May 1989

WGShafer

Dean, College of Engineering

Dean, Graduate School